LA-UR-19-26578
Approved for public release; distribution is unlimited.

Title: Analytic Solutions as a Tool for Verification and Validation of a Multiphysics Model: Application to the RMI+SSVD Ejecta Source Model

Author(s): Tregillis, Ian Lee

Intended for: Presentation to the biweekly XCP Division Seminar on Thursday, July 18, 2019.

Issued: 2019-07-11

Disclaimer:
Los Alamos National Laboratory, an affirmative action/equal opportunity employer, is operated by Triad National Security, LLC for the National Nuclear Security Administration of U.S. Department of Energy under contract 89233218CNA000001. By approving this article, the publisher recognizes that the U.S. Government retains nonexclusive, royalty-free license to publish or reproduce the published form of this contribution, or to allow others to do so, for U.S. Government purposes. Los Alamos National Laboratory requests that the publisher identify this article as work performed under the auspices of the U.S. Department of Energy. Los Alamos National Laboratory strongly supports academic freedom and a researcher's right to publish; as an institution, however, the Laboratory does not endorse the viewpoint of a publication or guarantee its technical correctness.

Analytic Solutions as a Tool for Verification and Validation of a Multiphysics Model:

Application to the RMI+SSVD Ejecta Source Model

Ian Tregillis, XCP-6

XCP Seminar

July 18, 2019

Managed by Triad National Security, LLC for the U.S. Department of Energy's NNSA

Many people have contributed to LANL ejecta studies.

FLAG Development & Support

*Alan Harrison (XCP-1)
Jimmy Fung (XCP-1)
Nick Denissen (XCP-1)
Mac Kenamond (XCP-1)
Daryl Grunau (XCP-1)
Johnny Collins (XCP-1)
Chris Rousculp (XCP-6)

Model Development

Jim Hammerberg (XCP-5)
Guy Dimonte(XCP-6)
Guillermo Terrones (XTD-SS)
Frank Cherne (M-9)
Matt Williams (XCP-3)
Malcolm Andrews (ASC/PEM)
Marianne Francois (ASC/PEM)
Susan Kurien (ASC/PEM)

Datasets & Experiment Expertise

*William Buttler (P-23) (also model development)
Russ Olson (P-23)
Grant Bazan (XTD-PRI)
Jeremy Danielson (P-23)
Danny Sorenson (P-23)
Martin Schauer (P-21)

Technical Discussions

Fred Wysocki (XCP-DO)
Carl Johnson (XTD-PRI)
Brandon Wilson (XCP-8)
Joanne Budizen (XCP-8)
Jonathan Regele (XCP-4)
Garry Maskaly (XCP-8)
Kyle Hickmann (XCP-8)

Funding & Institutional Support

Aaron Koskelo (XCP-8)
Kathy Prestridge (P-23)
Amy Bauer (XTD-NTA)

This talk draws from an extensively documented body of work.

- “(U) An Analytic Study of Piezoelectric Ejecta Mass Measurements,” Tregillis, LA-UR-17-21218
- “(U) An Analytic Examination of Piezoelectric Ejecta Mass Measurements,” Tregillis, *Proceedings of the 2016 NECDC* (also LA-UR-17-20814)
- “(U) Piezoelectric Ejecta Mass Measurements I: General Analytic Study,” Tregillis, *Weapons Review Letters*, **47-Ejecta**:90—99 LA-CP-18-00436 (2018)
- “(U) Piezoelectric Ejecta Mass Measurements II: Analytic Study of the RMI+SSVD Source Model,” Tregillis, *Weapons Review Letters*, **47-Ejecta**:100—109 LA-CP-18-00436 (2018)
- “(U) Piezoelectric Ejecta Mass Measurements III: Cross-Comparison of Theory, Simulation, & Experiment,” Tregillis, *Weapons Review Letters*, **47-Ejecta**:110—119 LA-CP-18-00436 (2018)
- “(U) Piezoelectric Ejecta Mass Measurements IV: Source Model Predictions for Thresholded Data,” Tregillis, *Weapons Review Letters*, **49**:62—71 LA-CP-18-00703 (2018)
- “(U) Boundary Conditions for Ejecta Source Models with Stationary Velocity Distributions,” Tregillis, LA-UR-18-27420
- “(U) Verification and Validation Studies of the RMI+SSVD Ejecta Source Model,” Tregillis, *Proceedings of the 2018 NECDC* (also LA-UR-18-31804)
- “Analytic Solutions as a Tool for Verification and Validation of a Multiphysics Model,” Tregillis & Koskelo, *Proceedings of the ASME 2019 Verification and Validation Symposium* (also LA-UR-19-20631v2)

Overview

- Introduction: “V & V is simply the scientific method…”
- Application: the RMI+SSVD Ejecta Source Model
  - The “Compatibility Score” Metric
- The (not so) Hidden Freshman Physics Problem
- Better Living Through Boundary Conditions
- Quantitative V & V: Our Guide to Future Efforts
  - Meta-analysis of >100,000 scenarios
- Summary: “V & V is simply the scientific method…”

“V&V is simply the scientific method for computational modeling and simulation.”

-- Bill Rider, SNL

A common challenge is to resolve ambiguities between issues of validation and issues of verification.

Simulations ← *Discrepancies beget ambiguities.* → **Data** (“reality”)

- **Validation issue?**
  - Does the physics model reflect reality?
- **Verification issue?**
  - Is the physics model implemented correctly?
  - Is the implementation numerically accurate?
- **Both? Neither?**
  - Is the simulation setup incorrect? Incomplete?
  - Are we outside the model’s domain of validity?
  - Is the dataset misapplied? Misinterpreted?
  - Did the dataset get corrupted in the repository?

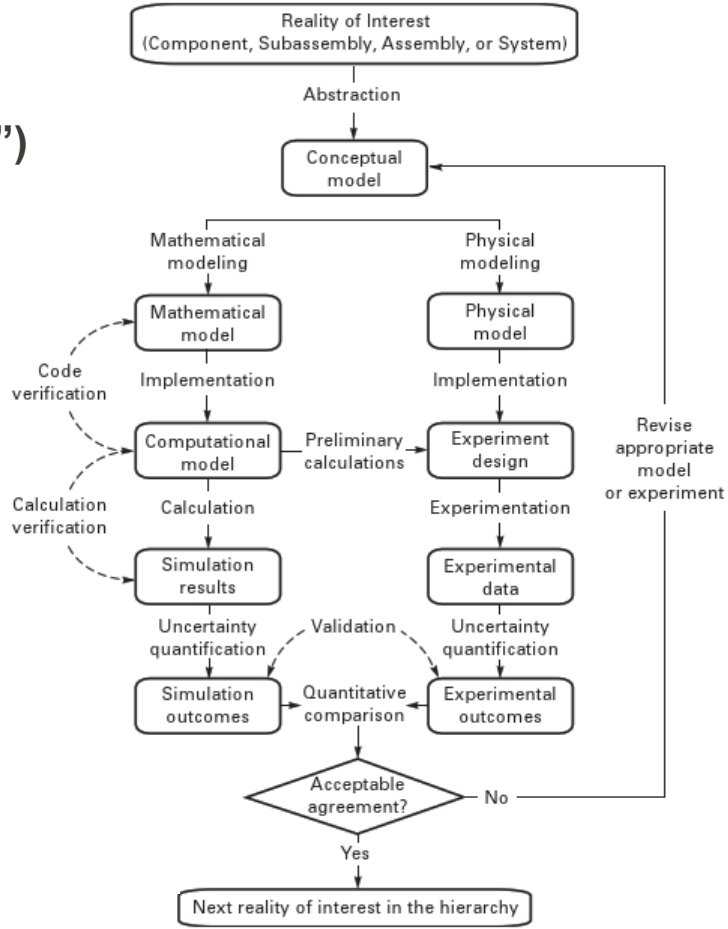

ASME V&V 10-2006, Fig. 4

This is particularly challenging when the model, and its numerical implementation, are active research topics.

Simulations ← *Discrepancies beget ambiguities.* → **Data** (“reality”)

- **Validation issue?**
  - Does the physics model reflect reality?
- **Verification issue?**
  - Is the physics model implemented correctly?
  - Is the implementation numerically accurate?
- **Both? Neither?**
  - Is the simulation setup incorrect? Incomplete?
  - Are we outside the model’s domain of validity?
  - Is the dataset misapplied? Misinterpreted?
  - Did the dataset get corrupted in the repository?

Once in a while, a complex multiphysics system may allow for a closed-form analytic solution.

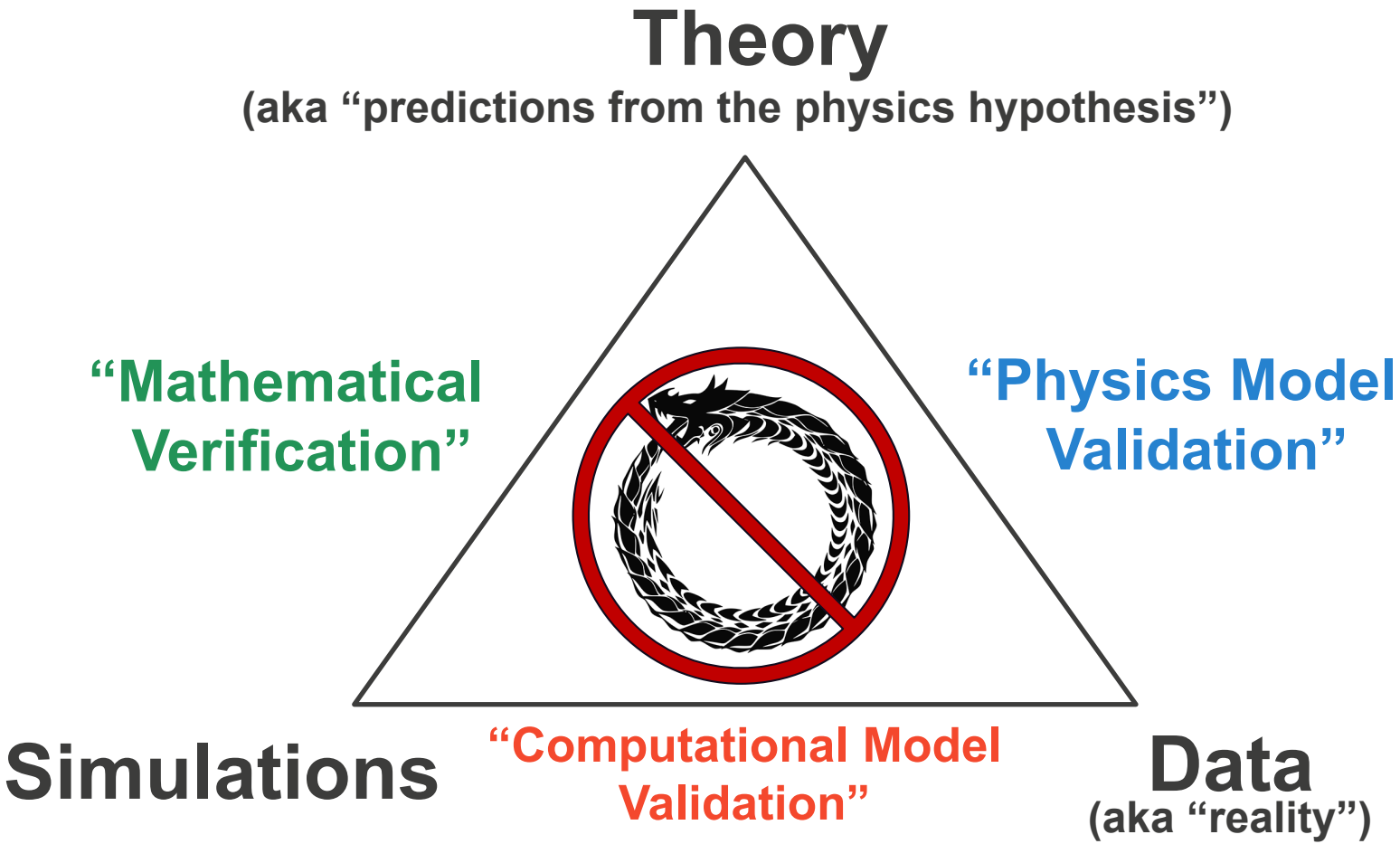

Once in a while, a complex multiphysics system may allow for a closed-form analytic solution.

- Simulation-data comparisons provide accuracy, uncertainties, & bounds on model utility.
  - Additional work is needed to identify the causes of these uncertainties and bounds.
- Theory-simulation comparisons tell us how the code performs relative to the model, and how to improve the code.
- Theory-data comparisons tell us how the model performs relative to the data, and how to improve the model.

Application: The RMI+SSVD Ejecta Source Model

The RMI+SSVD ejecta source model has been implemented as a sub-grid model in FLAG.

Example calculation: FLAG v 3.8.α.11
`numperptcl` = 10^2 ; `nsites` = 0 ; `floor_npackets` = 1

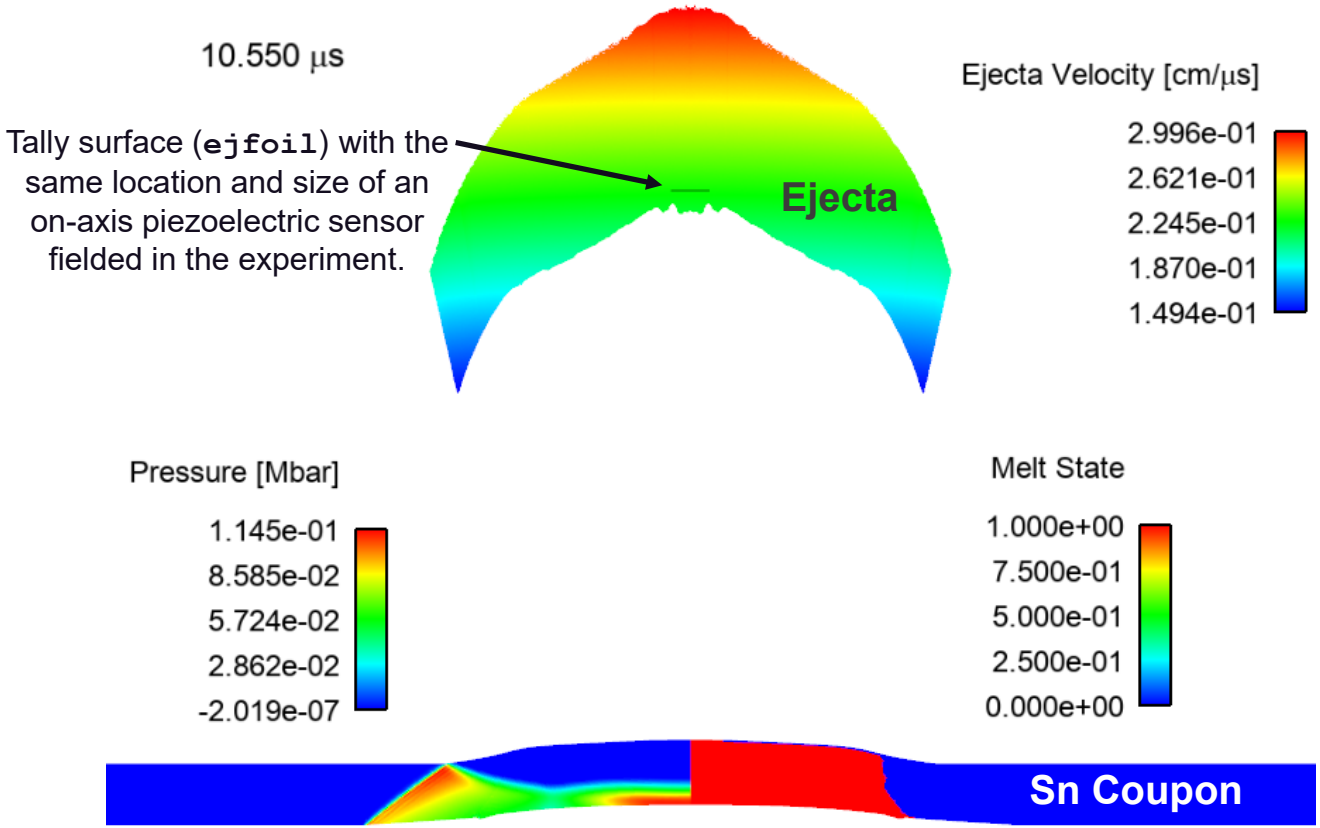

This capability has been applied to simulations of HE-driven, singly shocked tin coupon experiments conducted in vacuum:

Vogan et al. *J. Appl. Phys.* 98:113508 (2005)

Example image is taken from a calculation of Vogan shot 06.

*Fung et al., Computers & Fluids 83:177 (2013); Harrison, LA-UR-15-26632

Increasing the coupon thickness in FLAG relative to the fielded geometry yielded velocities and pressures consistent with the published experimental error bars.

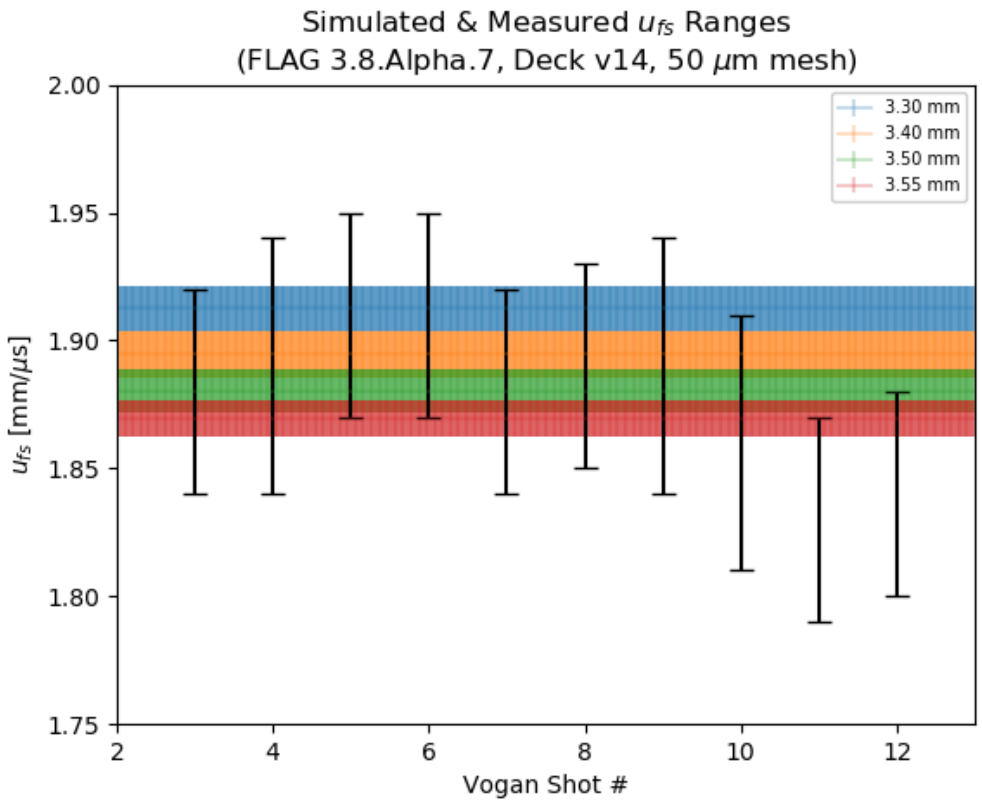

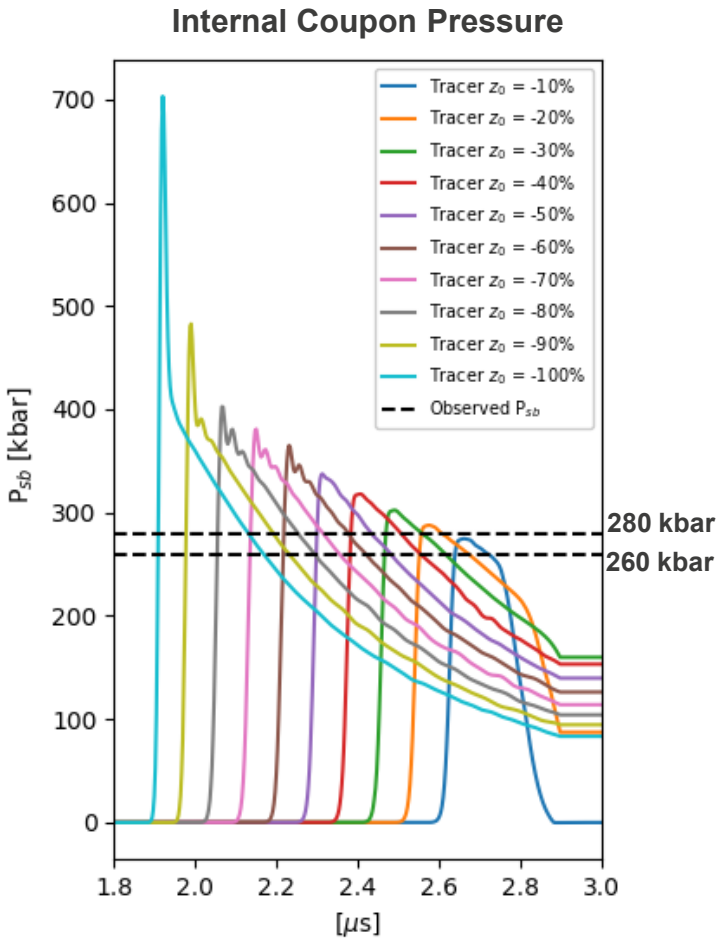

Vogan et al. *J. Appl. Phys.* 98:113508 (2005)

Piezoelectric sensor data (time-dependent ejecta mass inferred from piezo voltages) are crucial for assessing the model.

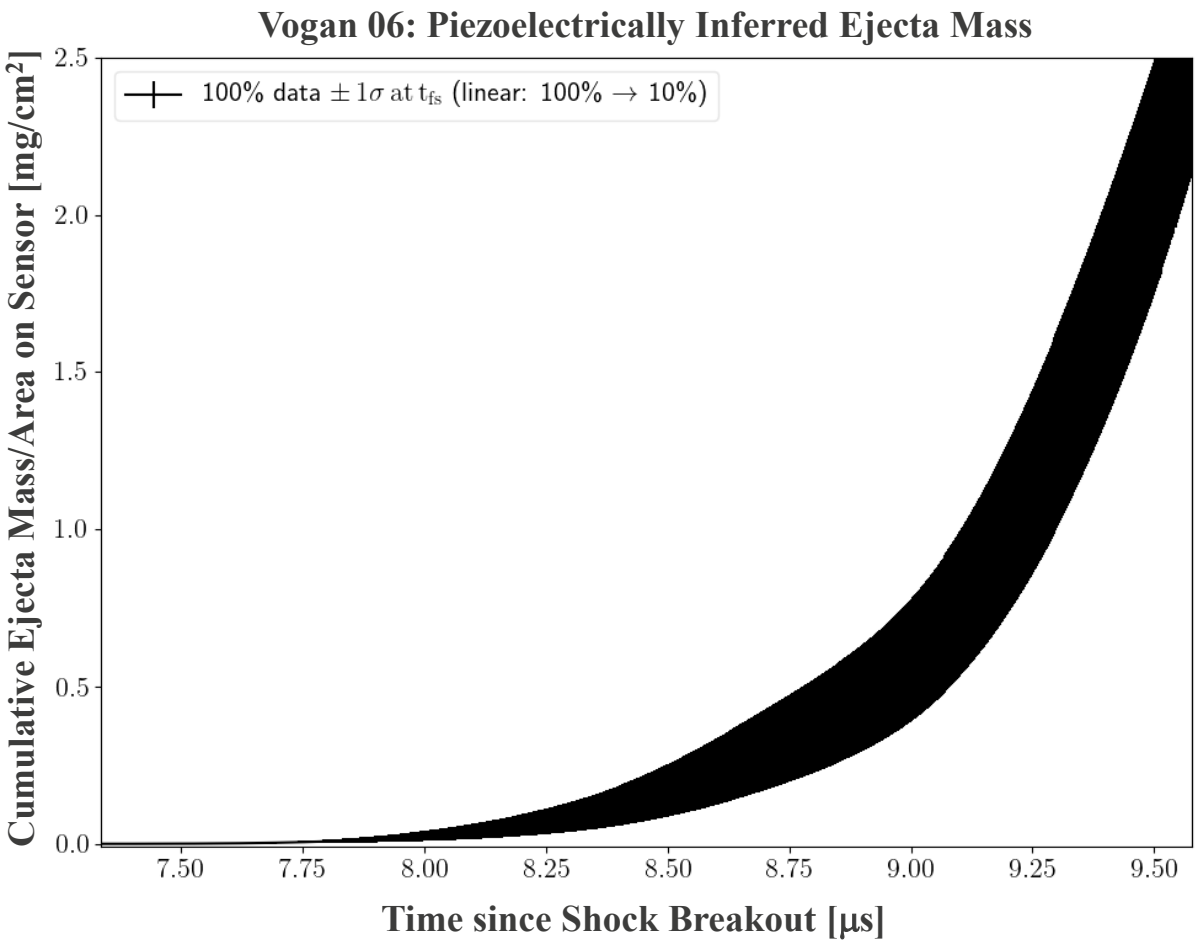

1σ uncertainty on data is ±10% at t_{fs}.*
Plotted error bars represent
±100% at t_{a0} → ±10% at t_{fs}

*Buttler et al. *J. Appl. Phys.* 101:063547 (2007);
Zellner et al. *J. Appl. Phys.* 103:123502 (2008);
Monfared et al. *J. Appl. Phys.* 116:063504 (2014)

Vogan et al. *J. Appl. Phys.* 98:113508 (2005); piezoelectric data courtesy of William Buttler.

FLAG `ejfoil` mass tallies are directly comparable to the piezoelectrically inferred ejecta mass data…

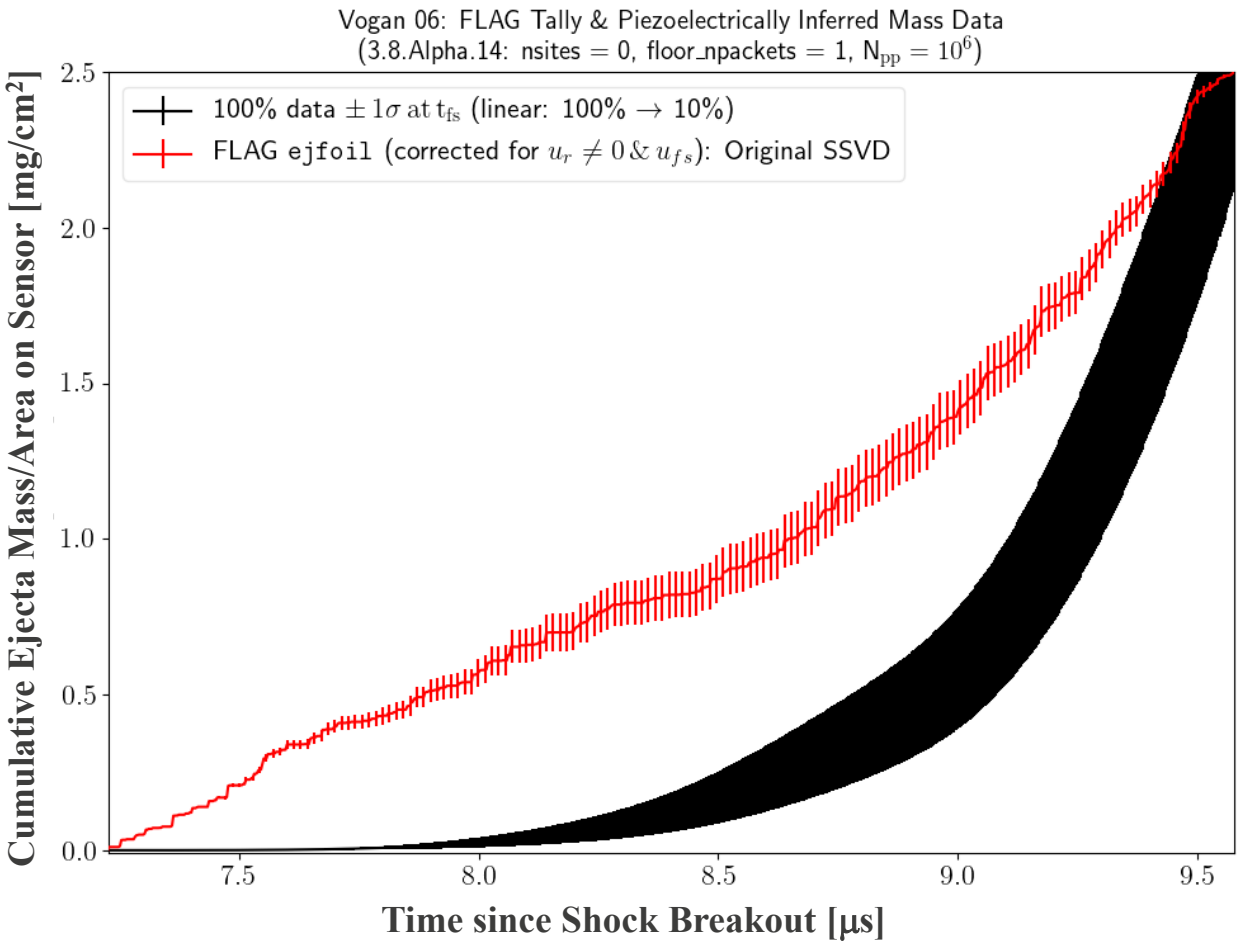

1σ uncertainty on data is ±10% at t_{fs}.*
Plotted error bars represent
±100% at t_{a0} → ±10% at t_{fs}

FLAG error bars derive from a Latin hypercube study of **`nsites`** & **`floor_npackets`**, combined with a separate study of **`numperptcl`** (3.8.α.12)

*Buttler et al. *J. Appl. Phys.* 101:063547 (2007); Zellner et al. *J. Appl. Phys.* 103:123502 (2008); Monfared et al. *J. Appl. Phys.* 116:063504 (2014)

Vogan et al. *J. Appl. Phys.* 98:113508 (2005); piezoelectric data courtesy of William Buttler.

…but doing so tells us very little about the underlying ejecta source model.

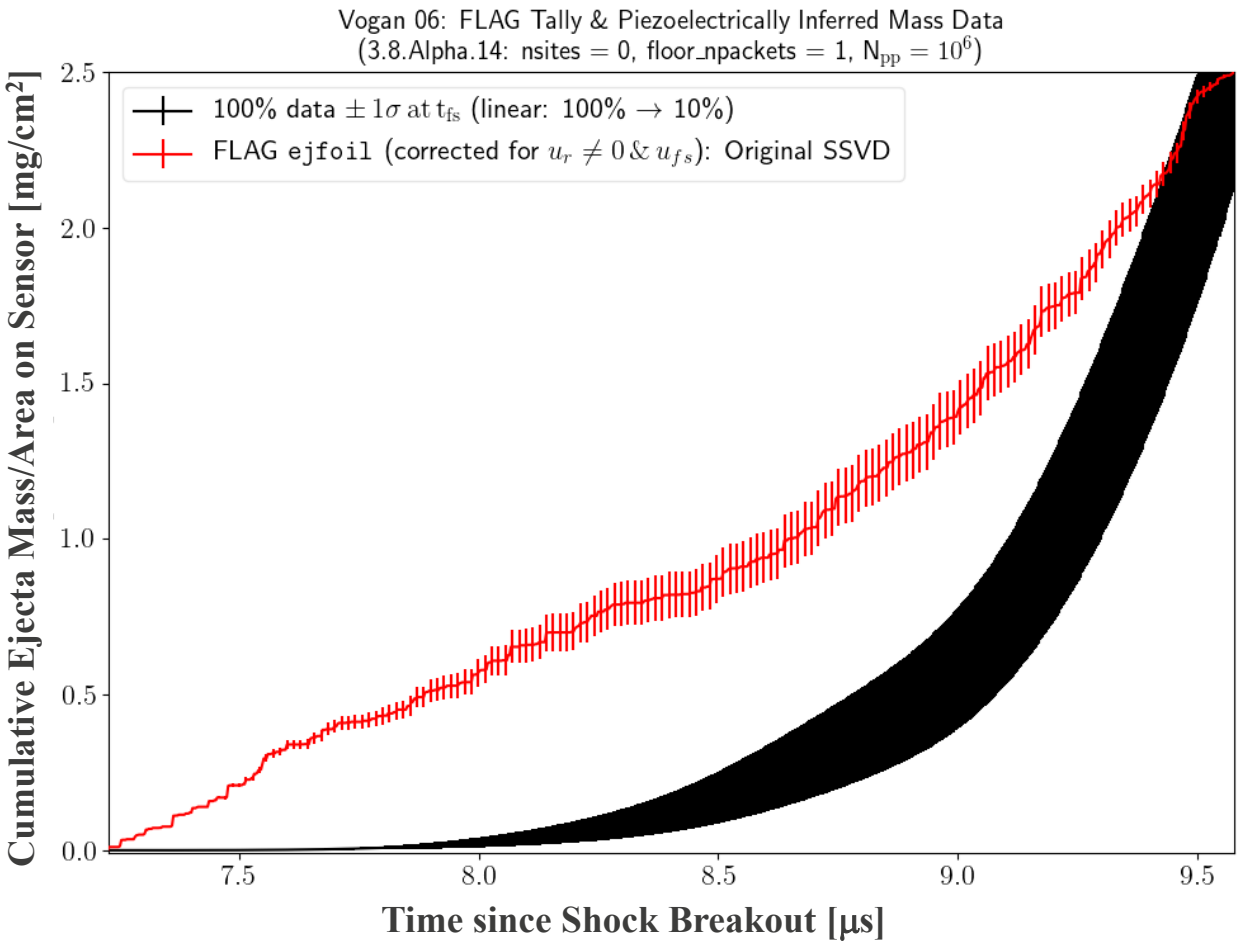

To improve our predictive capability, should we invest in:

- **Code development?**
- **Model development?**
- **Both?**
- **Neither?**

Vogan et al. *J. Appl. Phys.* 98:113508 (2005); piezoelectric data courtesy of William Buttler.

…but doing so tells us very little about the underlying ejecta source model.

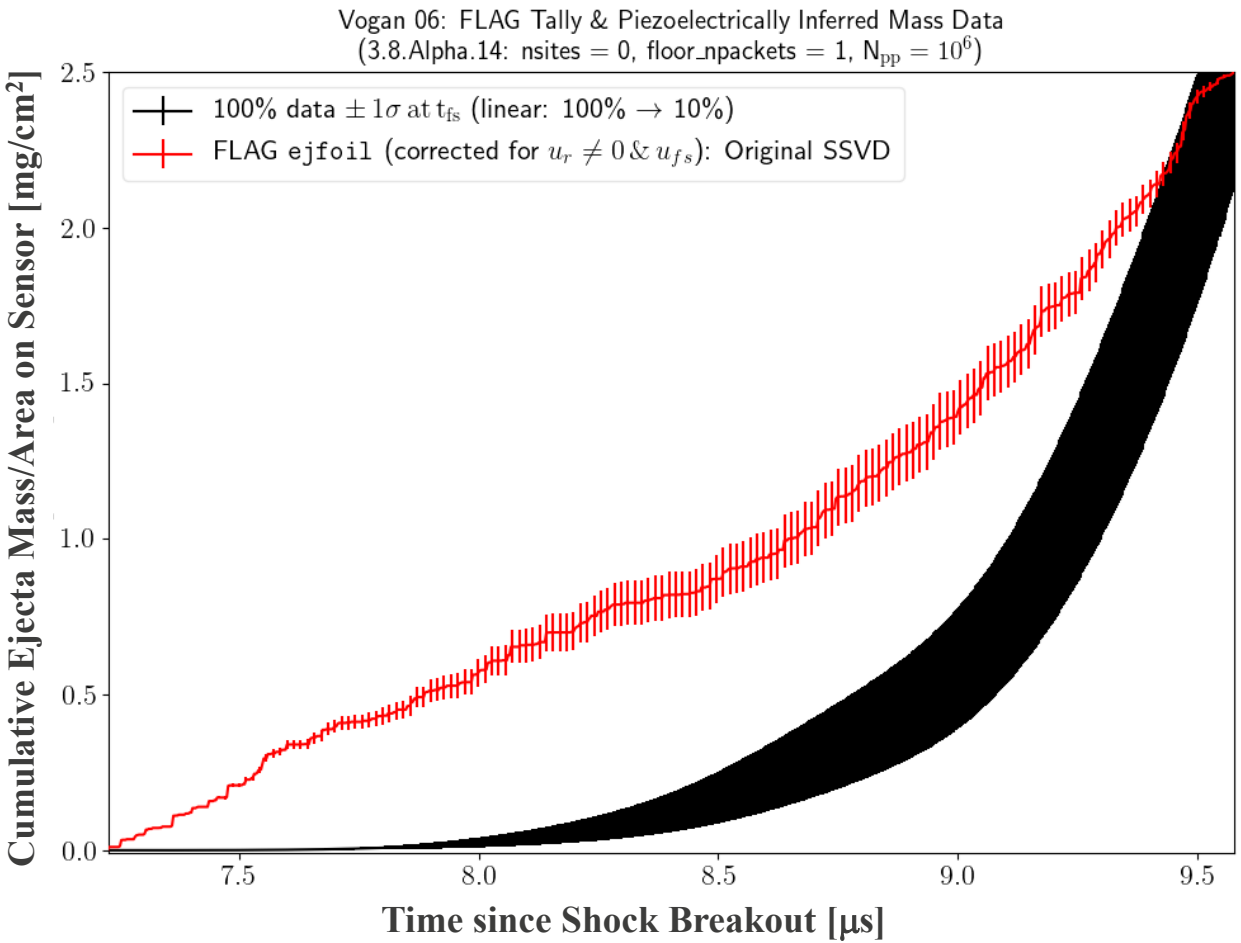

To improve our predictive capability, should we invest in:

- **Code development?**
- **Model development?**
- **Both?**
- **Neither?**

How can we address these questions unless we know what the <u>underlying</u> <u>model</u> predicts?

Vogan et al. *J. Appl. Phys.* 98:113508 (2005); piezoelectric data courtesy of William Buttler.

These investigations are made quantitative through the introduction of the "compatibility score" metric.

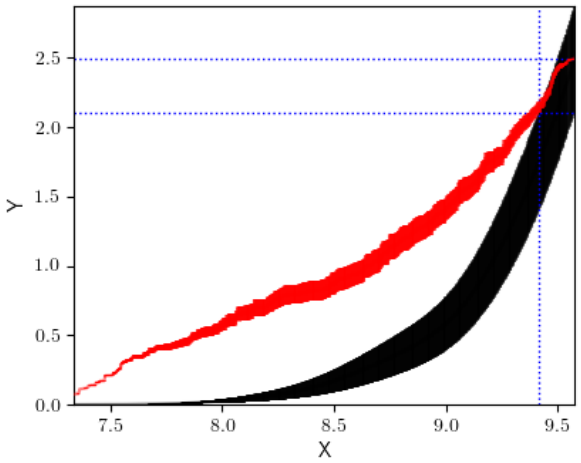

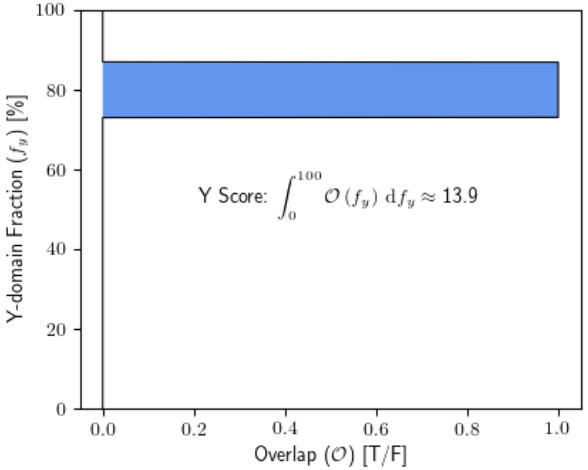

Q: Over what percentage of the physics domain of interest do two curves overlap?

A: The compatibility score is a scalar value in [0, 100].

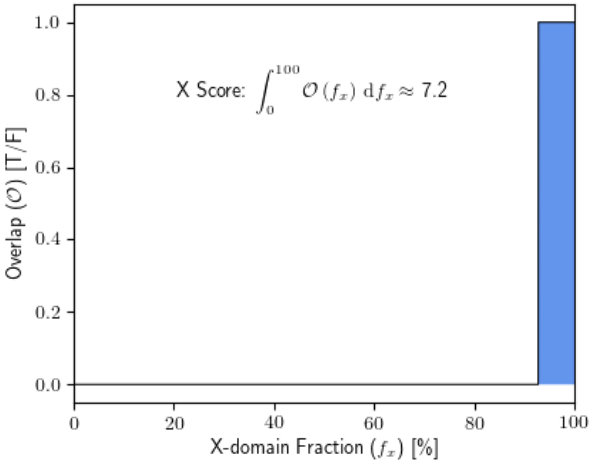

For time-dependent piezoelectrically inferred ejecta mass data:

- x-score = fraction of the ejecta-arrival time interval
- y-score = fraction of the total mass delivered to the sensor

The Vogan 06 FLAG/data comparisons shown here & on the previous slide have a mass compatibility score of ~14%.

Vogan et al. *J. Appl. Phys.* 98:113508 (2005); piezoelectric data courtesy of William Buttler.

Thresholding the data isn't a panacea.

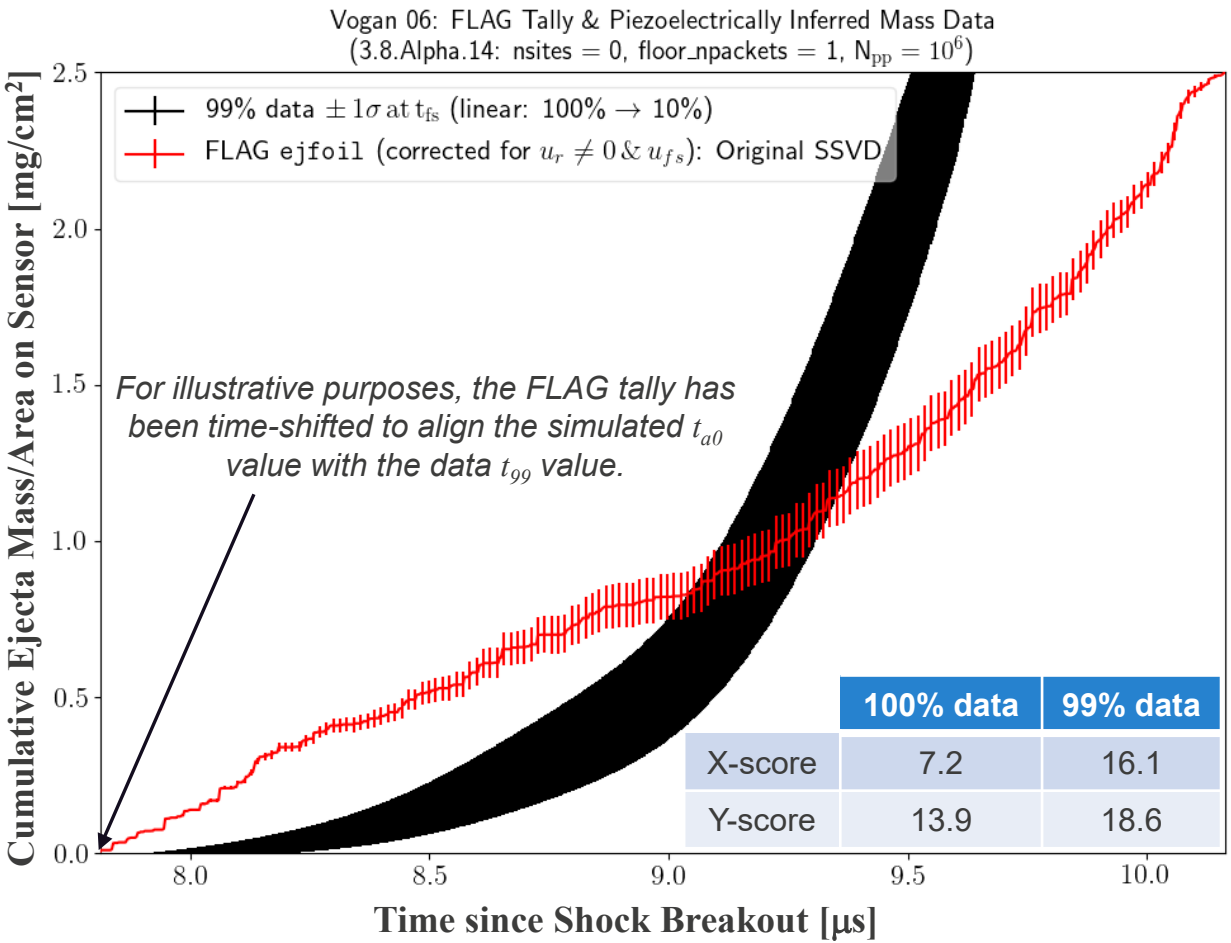

	100% data	99% data
X-score	7.2	16.1
Y-score	13.9	18.6

"The model targets 99% of the mass."

- Thresholding out the earliest-arriving 1% of the ejecta mass shortens the targeted data arrival interval by ~0.6 μs for this shot.
- Meanwhile, the simulated data arrival interval does not change.
- The simulated arrival interval is a far better match to the full dataset.
- Superior results can be obtained by restricting our attention to the full (100%) dataset, as shown below.

Vogan et al. *J. Appl. Phys.* 98:113508 (2005); piezoelectric data courtesy of William Buttler.

The (not so) Hidden Freshman Physics Problem

Fair play: let's proceed using <u>only</u> the assumptions intrinsic to the piezo analysis procedure.

When

- all ejecta are created instantaneously at shock breakout,
- all ejecta motion is collinear, with a long m.f.p. to scattering,
- all ejecta particles have constant velocity while in transit,
- all ejecta particles collide perfectly inelastically with the sensor,
- the ejecta cloud contains no mass sinks or sources, and
- the piezoelectric sensor is driven in a linear regime

then the raw voltage measurement is simply related to dynamical properties of the ejecta cloud (cumulative mass).*

Here we drop the instant-creation requirement and study the case $\dot{u_{fs}} = 0$†.

*Buttler et al. *J. Appl. Phys.* 116:103519 (2014)

†Monfared et al. *J. Appl. Phys.* 116:063504 (2014)

Some of the most valuable data for this problem comprise piezo measurements of planar, single-shock ejection into vacuum…

...or, in other words, a

one-dimensional

vacuum

kinematics problem.

At heart, this is a freshman physics problem!

1D vacuum kinematics establishes the relationship between creation time, measurement time, and velocity for any particle.

- Consider a surface accelerated instantaneously* to lab-frame velocity u_{fs} at time t_0.
- At time t_c, this surface emits a particle with relative velocity w (lab-frame $u = w + u_{fs}$).
- That particle arrives at the sensor at measurement time t.

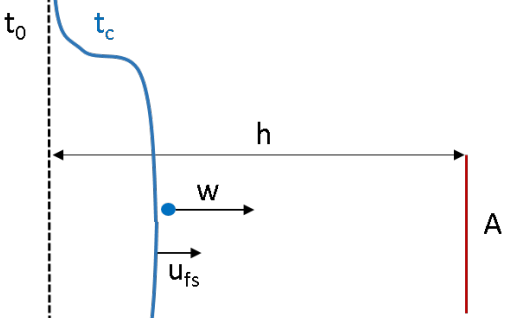

$$t\left(w, t_c\right) = t_c + \frac{h - u_{fs}\left(t_c - t_0\right)}{w + u_{fs}} = \frac{w t_c + \left(h + u_{fs} t_0\right)}{w + u_{fs}}$$

$$t_c\left(w, t\right) = \frac{\left(w + u_{fs}\right) t - \left(h + u_{fs} t_0\right)}{w}$$

$$\frac{dt}{dt_c} = \left(\frac{w}{w + u_{fs}}\right) = \left(\frac{u - u_{fs}}{u}\right)$$

$$\frac{dt_c}{dt} = \left(\frac{w + u_{fs}}{w}\right) = \left(\frac{u}{u - u_{fs}}\right)$$

*Monfared et al. *J. Appl. Phys.* 116:063504 (2014)

Defining an "areal mass function" enables us to derive source model predictions for the piezoelectric data in these experiments.

Particles are created at the free surface with time-dependent mass & velocity distributions:

$$f_c\left(m, w, t_c\right) \mathrm{d}m \, \mathrm{d}w \, \mathrm{d}t_c$$

The source Areal Mass Function is the 1st mass moment of that distribution:

$$\boxed{m_c\left(w, t_c\right) \equiv \frac{1}{A} \int m f_c\left(m, w, t_c\right) \mathrm{d}m}$$

(source physics hypothesis lives here)

The true mass accumulation on the sensor (in a perfect system) follows directly:

$$m_t(t) = \int_{\frac{h}{t} - u_{fs}}^{\infty} \mathrm{d}w \int_0^{t_c(w,t)} m_c(w, t_c') \, \mathrm{d}t_c'$$

One can also derive the epistemic uncertainty in the piezoelectrically inferred mass:

$$\Delta m(t) = \frac{1}{h} \int_{\frac{h}{t} - u_{fs}}^{\infty} w \, \mathrm{d}w \int_0^{t_c(w,t)} t_c' \, m_c(w, t_c') \, \mathrm{d}t_c'$$

as well as the model prediction for the raw piezoelectric voltage:

$$V \propto \frac{dP}{dt} \qquad P\left(t\right) = \int_0^{\infty} m_a\left(u, t\right) u \, \mathrm{d}u = \int_0^{\infty} \left(\frac{u^2}{u - u_{fs}}\right) m_c\left[u - u_{fs}, \frac{ut - \left(h + u_{fs} t_0\right)}{u - u_{fs}}\right] \mathrm{d}u$$

The SSVD is well-approximated by a stationary distribution. Then the RMI+SSVD model is described by a simple source AMF…

$$m_c(w,t_c) = \frac{2}{3} m_0 \cdot \frac{1}{t_c + \beta\tau} \cdot \frac{\xi e^{-\frac{\xi w}{\dot{\eta}^s}} + 1}{(2 - e^{-\xi})\dot{\eta}^s} \cdot \prod_0^{t_{cf}}(t_c)$$

…from which we obtain expressions for m_t and Δm.

$$m_c(w,t_c) = \frac{2}{3} m_0 \cdot \frac{1}{t_c + \beta\tau} \cdot \frac{\xi e^{-\frac{\xi w}{\dot\eta^s}} + 1}{(2 - e^{-\xi})\dot\eta^s} \cdot \prod_0^{t_{cf}}(t_c)$$

$$m_t(t) = \begin{cases} \dfrac{2m_0\xi}{3\dot\eta^s(2-e^{-\xi})} \displaystyle\int_{\frac{h}{t}-u_{fs}}^{\frac{h-u_{fs}t}{t-t_{cf}}} e^{-\frac{\xi w}{\dot\eta^s}} \ln\left[p(t) + \frac{q(t)}{w}\right] dw \\ + \dfrac{2m_0}{3\dot\eta^s(2-e^{-\xi})} \displaystyle\int_{\frac{h}{t}-u_{fs}}^{\frac{h-u_{fs}t}{t-t_{cf}}} \ln\left[p(t) + \frac{q(t)}{w}\right] dw \\ + \dfrac{2m_0\xi}{3\dot\eta^s(2-e^{-\xi})} \ln\left(1 + \frac{t_{cf}}{\beta\tau}\right) \displaystyle\int_{\frac{h-u_{fs}t}{t-t_{cf}}}^{\dot\eta^s} e^{-\frac{\xi w}{\dot\eta^s}} dw \\ + \dfrac{2m_0}{3\dot\eta^s(2-e^{-\xi})} \ln\left(1 + \frac{t_{cf}}{\beta\tau}\right) \displaystyle\int_{\frac{h-u_{fs}t}{t-t_{cf}}}^{\dot\eta^s} dw & (t > t^*) \\ \\ \dfrac{2m_0\xi}{3\dot\eta^s(2-e^{-\xi})} \displaystyle\int_{\frac{h}{t}-u_{fs}}^{\dot\eta^s} e^{-\frac{\xi w}{\dot\eta^s}} \ln\left[p(t) + \frac{q(t)}{w}\right] dw \\ + \dfrac{2m_0}{3\dot\eta^s(2-e^{-\xi})} \displaystyle\int_{\frac{h}{t}-u_{fs}}^{\dot\eta^s} \ln\left[p(t) + \frac{q(t)}{w}\right] dw & (t \le t^*) \end{cases}$$

$$\Delta m(t) = \begin{cases} \dfrac{2m_0\beta\tau\xi}{3\dot\eta_s h} \cdot \dfrac{[p(t)-1]}{2-e^{-\xi}} \displaystyle\int_{\frac{h}{t}-u_{fs}}^{\frac{h-u_{fs}t}{t-t_{cf}}} w e^{-\frac{\xi w}{\dot\eta_s}} dw \\ + \dfrac{2m_0\beta\tau\xi}{3\dot\eta_s h} \cdot \dfrac{q(t)}{2-e^{-\xi}} \displaystyle\int_{\frac{h}{t}-u_{fs}}^{\frac{h-u_{fs}t}{t-t_{cf}}} e^{-\frac{\xi w}{\dot\eta_s}} dw \\ - \dfrac{2m_0\beta\tau\xi}{3\dot\eta_s h(2-e^{-\xi})} \displaystyle\int_{\frac{h}{t}-u_{fs}}^{\frac{h-u_{fs}t}{t-t_{cf}}} w e^{-\frac{\xi w}{\dot\eta_s}} \ln\left[p(t) + \frac{q(t)}{w}\right] dw \\ + \dfrac{2m_0\beta\tau}{3\dot\eta_s h} \cdot \dfrac{[p(t)-1]}{2-e^{-\xi}} \displaystyle\int_{\frac{h}{t}-u_{fs}}^{\frac{h-u_{fs}t}{t-t_{cf}}} w dw \\ + \dfrac{2m_0\beta\tau}{3\dot\eta_s h} \cdot \dfrac{q(t)}{2-e^{-\xi}} \displaystyle\int_{\frac{h}{t}-u_{fs}}^{\frac{h-u_{fs}t}{t-t_{cf}}} dw \\ - \dfrac{2m_0\beta\tau}{3\dot\eta_s h(2-e^{-\xi})} \displaystyle\int_{\frac{h}{t}-u_{fs}}^{\frac{h-u_{fs}t}{t-t_{cf}}} w \ln\left[p(t) + \frac{q(t)}{w}\right] dw \\ + \dfrac{2m_0\xi}{3\dot\eta_s h(2-e^{-\xi})} \cdot \left[t_{cf} - \beta\tau\ln\left(1 + \frac{t_{cf}}{\beta\tau}\right)\right] \displaystyle\int_{\frac{h-u_{fs}t}{t-t_{cf}}}^{\dot\eta_s} w e^{-\frac{\xi w}{\dot\eta_s}} dw \\ + \dfrac{2m_0}{3\dot\eta_s h(2-e^{-\xi})} \cdot \left[t_{cf} - \beta\tau\ln\left(1 + \frac{t_{cf}}{\beta\tau}\right)\right] \displaystyle\int_{\frac{h-u_{fs}t}{t-t_{cf}}}^{\dot\eta_s} w dw & t > t^* \\ \\ \dfrac{2m_0\beta\tau\xi}{3\dot\eta_s h} \cdot \dfrac{[p(t)-1]}{2-e^{-\xi}} \displaystyle\int_{\frac{h}{t}-u_{fs}}^{\dot\eta_s} w e^{-\frac{\xi w}{\dot\eta_s}} dw \\ + \dfrac{2m_0\beta\tau\xi}{3\dot\eta_s h} \cdot \dfrac{q(t)}{2-e^{-\xi}} \displaystyle\int_{\frac{h}{t}-u_{fs}}^{\dot\eta_s} e^{-\frac{\xi w}{\dot\eta_s}} dw \\ - \dfrac{2m_0\beta\tau\xi}{3\dot\eta_s h(2-e^{-\xi})} \displaystyle\int_{\frac{h}{t}-u_{fs}}^{\dot\eta_s} w e^{-\frac{\xi w}{\dot\eta_s}} \ln\left[p(t) + \frac{q(t)}{w}\right] dw \\ + \dfrac{2m_0\beta\tau}{3\dot\eta_s h} \cdot \dfrac{[p(t)-1]}{2-e^{-\xi}} \displaystyle\int_{\frac{h}{t}-u_{fs}}^{\dot\eta_s} w dw \\ + \dfrac{2m_0\beta\tau}{3\dot\eta_s h} \cdot \dfrac{q(t)}{2-e^{-\xi}} \displaystyle\int_{\frac{h}{t}-u_{fs}}^{\dot\eta_s} dw \\ - \dfrac{2m_0\beta\tau}{3\dot\eta_s h(2-e^{-\xi})} \displaystyle\int_{\frac{h}{t}-u_{fs}}^{\dot\eta_s} w \ln\left[p(t) + \frac{q(t)}{w}\right] dw & t \le t^* \end{cases}$$

$$p(t) \equiv 1 + \frac{t}{\beta\tau}$$

$$q(t) \equiv \frac{u_{fs}t - h}{\beta\tau}$$

$$t^* \equiv \frac{h + \dot\eta^s t_{cf}}{\dot\eta^s + u_{fs}}$$

These expressions are not coded into FLAG.

This is a framework for <u>mathematical verification</u>.

We derive approximate uncertainty bounds on the model predictions from known experimental uncertainties.

Uncertainty	Source
$\sigma_h = 25\ \mu\text{m}$	Vogan et al., Tab. I caption
$\sigma_\Omega = 0.5$ Ohms	LeCroy LT374 data sheet
$\sigma_A = 0.1\ \text{mm}^2$	Computed using a pin radius uncertainty σ_h^*
$\sigma_S = 1.55$ pC/N	Vogan et al., § I†
$\sigma_{t_0} = 0.216\ \mu\text{s}$	Vogan et al., § III.A‡

These calculations don't incorporate $\sigma_{u_{fs}}$.

*Blind estimate.
†Derived from range of literature and manufacturer values.
‡Shock-breakout uncertainty + overall timing jitter.

$$\sigma_{m_i} \approx \sqrt{\left(\frac{\partial m}{\partial h}\sigma_h\right)^2 + \left(\frac{\partial m}{\partial A}\sigma_A\right)^2 + \left(\frac{\partial m}{\partial t_0}\sigma_{t_0}\right)^2 + \left(\frac{\partial m}{\partial \Omega}\sigma_\Omega\right)^2 + \left(\frac{\partial m}{\partial S}\sigma_S\right)^2}$$

$$\sigma_{m_t} \approx \sqrt{\left(\frac{\partial m}{\partial h}\sigma_h\right)^2 + \left(\frac{\partial m}{\partial A}\sigma_A\right)^2 + \left(\frac{\partial m}{\partial t_0}\sigma_{t_0}\right)^2}$$

m_i= piezo-<u>inferred</u> mass accumulation
m_t= <u>true</u> mass accumulation

Vogan et al. *J. Appl. Phys.* 98:113508 (2005)

Comparing FLAG tally surface output to piezopin data told us little about the underlying ejecta source model…

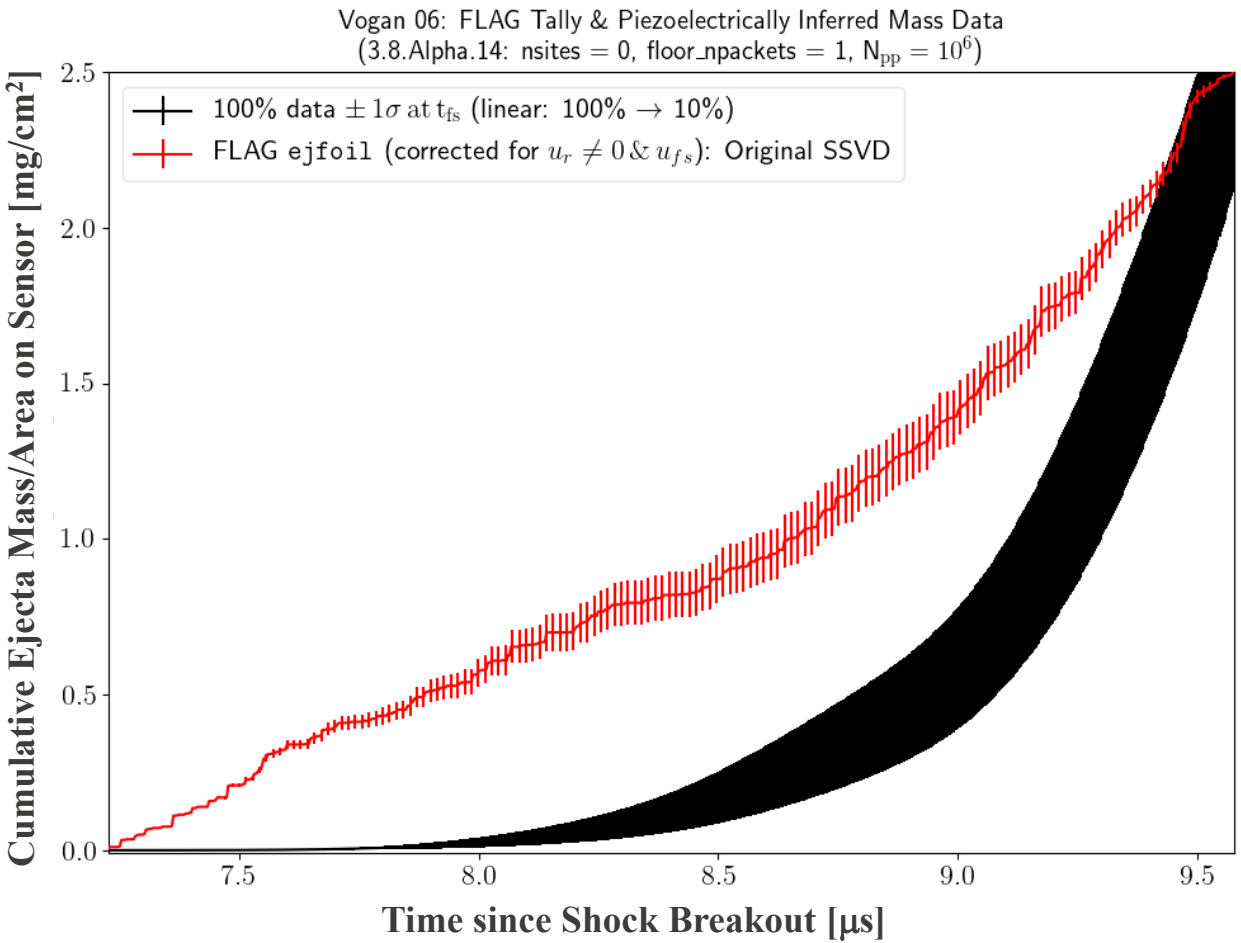

Vogan et al. *J. Appl. Phys.* 98:113508 (2005); piezoelectric data courtesy of William Buttler.

…but adding the analytic model prediction tells us the discrepancy is primarily a validation issue, not a verification issue.

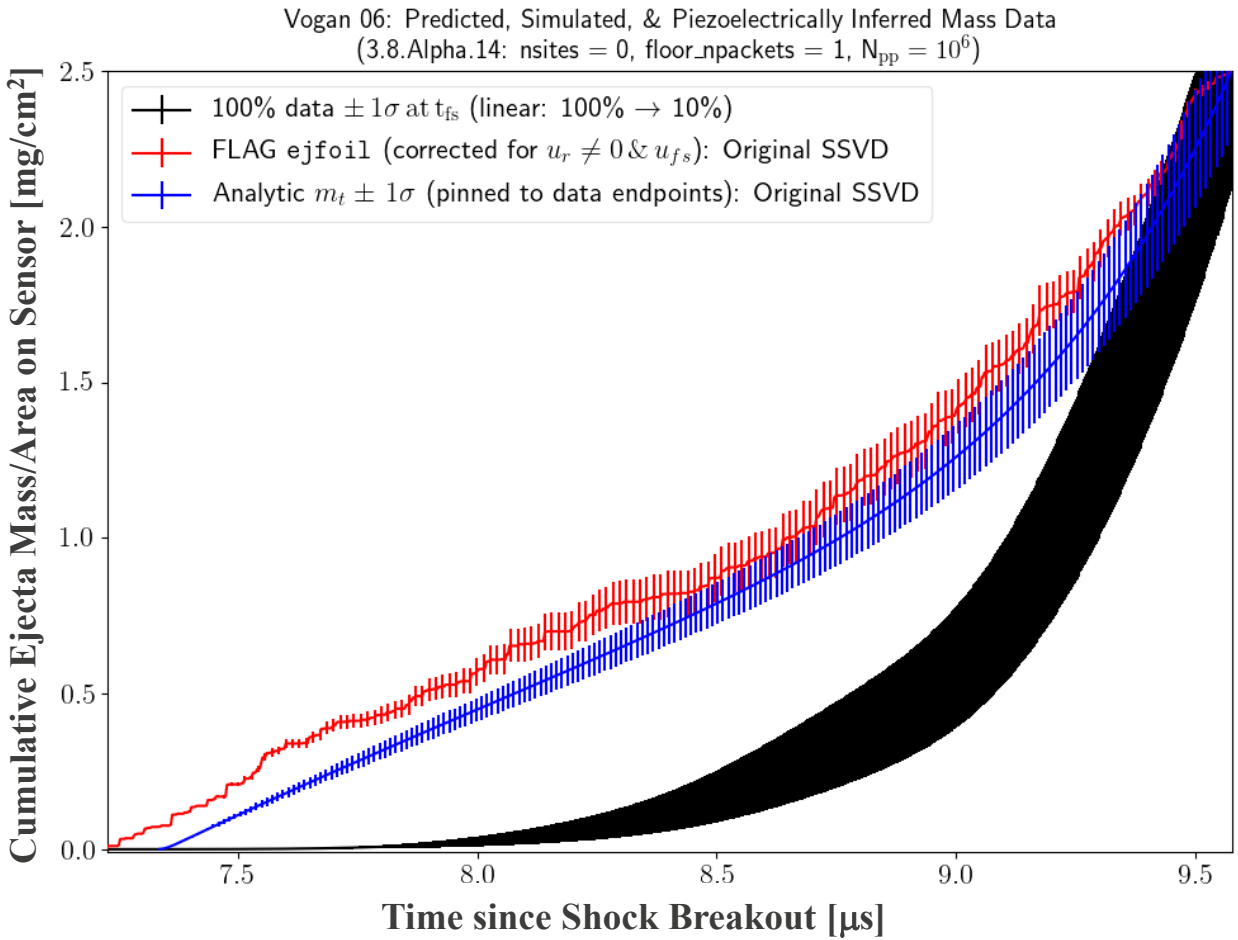

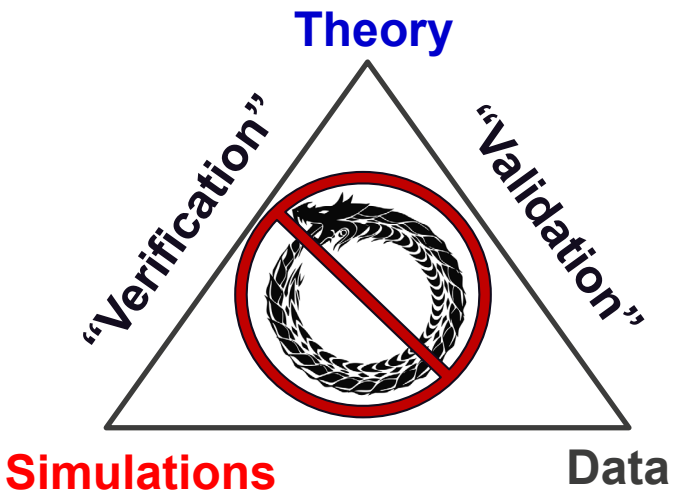

	Score
FLAG / 100% data	13.9
Theory / 100% data	39.7
FLAG / Theory	64.9

Vogan et al. *J. Appl. Phys.* 98:113508 (2005); piezoelectric data courtesy of William Buttler.

Better Living Through Boundary Conditions

Piezoelectric voltage datasets from these and related experiments exhibit two apparently global properties.

The time-dependent voltages:

- rise smoothly from the baseline
- are continuous.

These properties encode requirements for the model prediction, including:

- $V(t_{a0}) = 0$
- $V'(t_{a0}) = 0$
- $\lim_{\acute{t} \to t^-} V(\acute{t}) = \lim_{\acute{t} \to t^+} V(\acute{t}) \ \forall \ t$

where t_{a0} is the time of first arrival at the sensor.

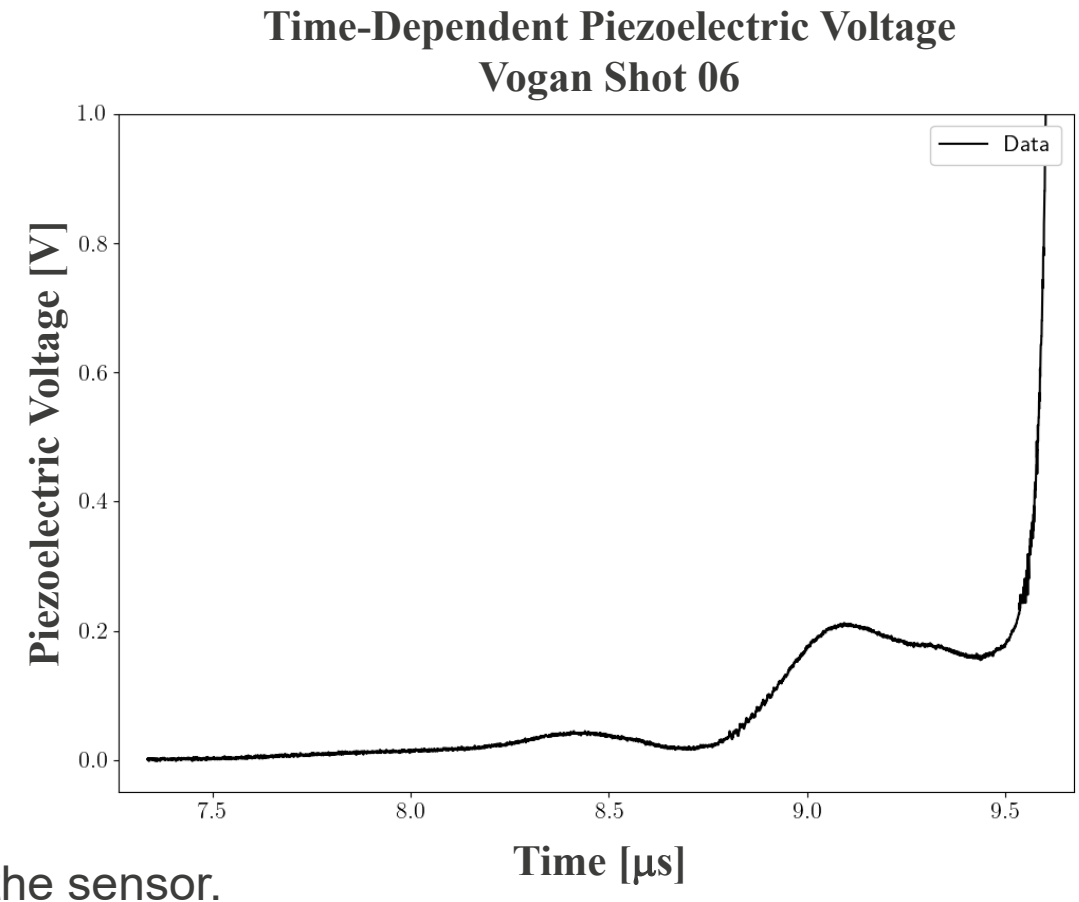

*Vogan et al. *J. Appl. Phys.* 98:113508 (2005); piezoelectric data courtesy of William Buttler.

These requirements constrain the boundary conditions for an <u>entire class</u> of ejecta source models.

Any source model with a stationary velocity distribution can be written

$$m_c(w, t_c) = m_0\, g(t_c)\, f(w) \prod_{t_0}^{t_{cf}} (t_c)$$

(Boxcar function enforces a "shut off" time, t_{cf})

Only certain boundary condition combinations will produce voltage predictions consistent with the preceding requirements:*

- $g(0) = f(\hat{w}) = 0$
- $f(\hat{w}) = f'(\hat{w}) = 0$:
- $g(0) = g'(0) = g(t_{cf}) = 0$

($\widehat{w}$ = max. relative ejecta velocity)

The RMI+SSVD source model

$$g(t_c) = \frac{2}{3}\frac{1}{t_c + \beta'\tau} \qquad f(w) = \frac{\xi e^{-\frac{\xi w}{\hat{w}}} + 1}{(2 - e^{-\xi})\hat{w}}$$

satisfies none of these conditions except $f'(\widehat{w}) \approx 0$ for suitably large ξ.

*Tregillis, LA-UR-18-27420

And indeed, the RMI+SSVD source model predicts an aberrant voltage trace.

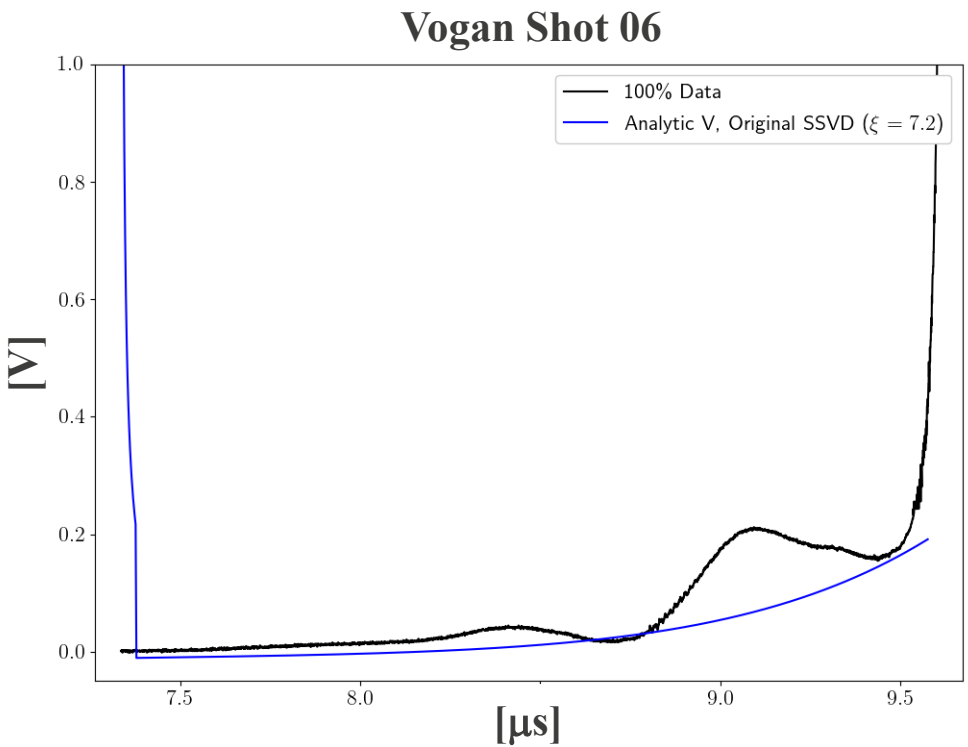

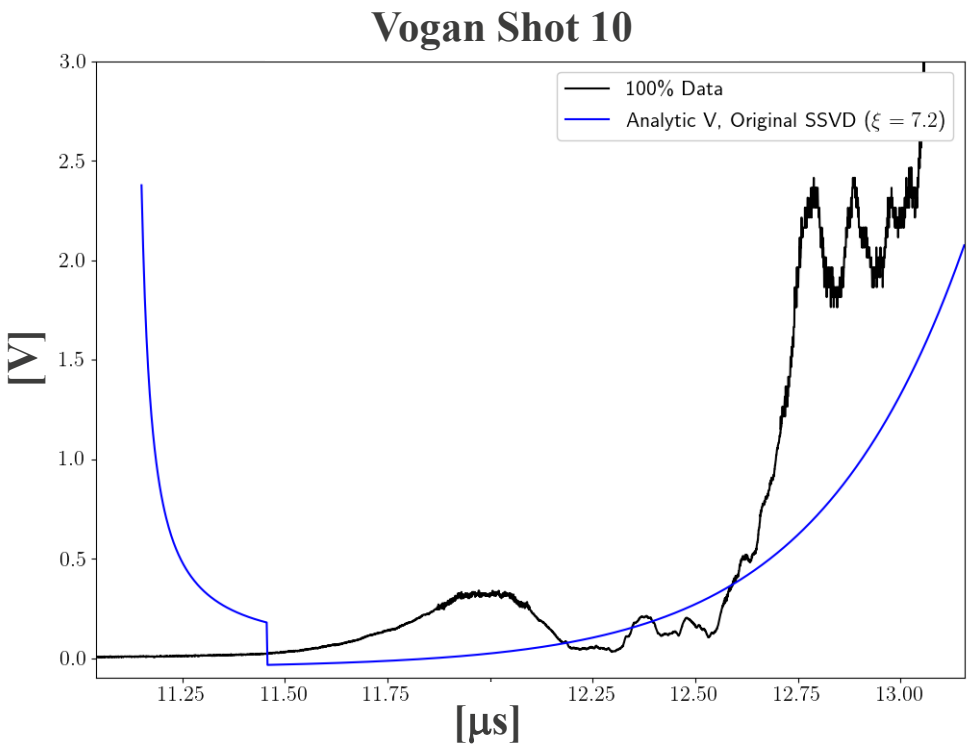

- **ANY** source model in this class will exhibit these problems if it violates the required BCs.
- These problems **ARE NOT CAUSED** by attempting to fit nuances of the data.
- Thresholding the data **DOES NOT CHANGE** this result.

*Vogan et al. *J. Appl. Phys.* 98:113508 (2005); piezoelectric data courtesy of William Buttler.

Fortunately, the derived boundary conditions can be satisfied with a simple modification to the original SSVD.

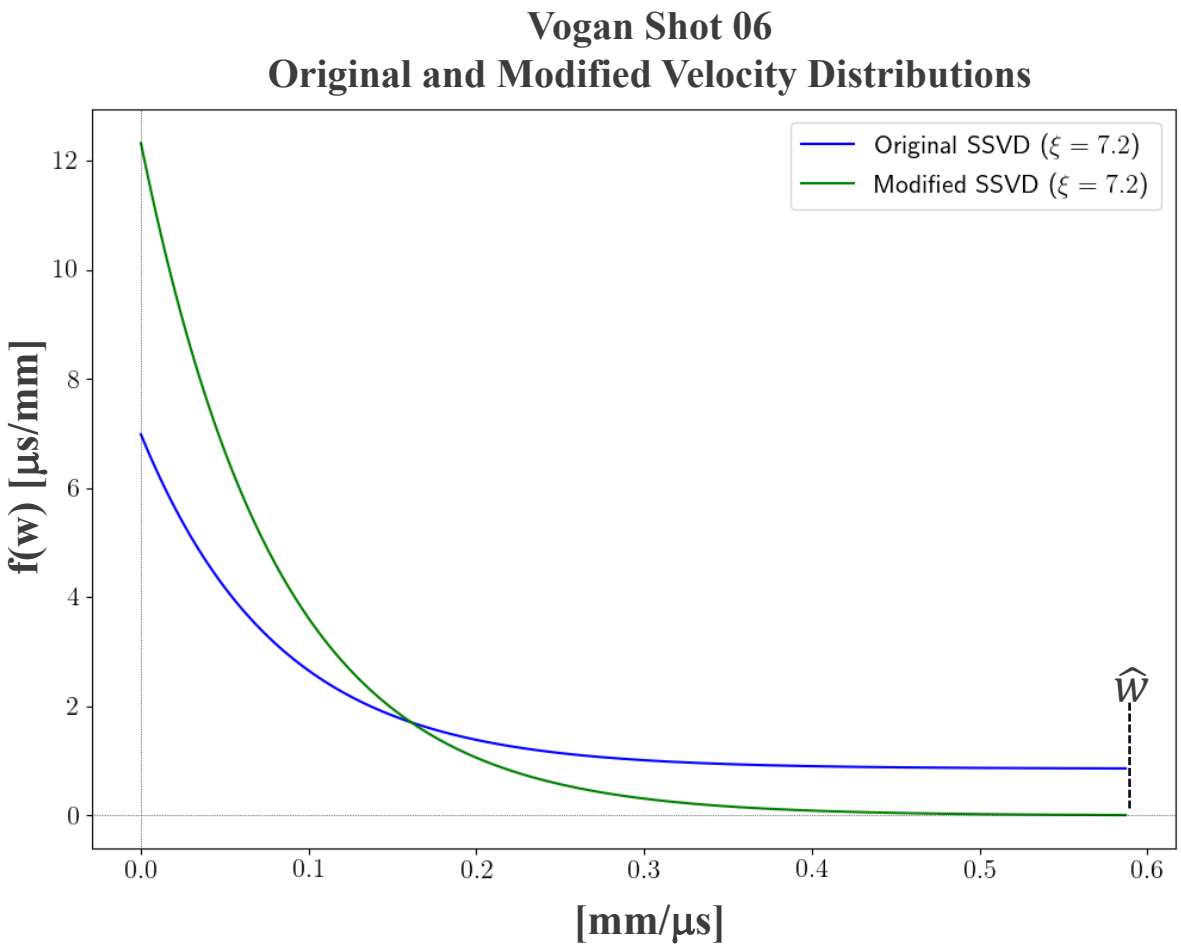

The original SSVD has

$$f(\widehat{w}) \neq 0$$
$$f'(\widehat{w}) \approx 0$$

We construct a new function

$$\tilde{f}(w) = \kappa[f(w) - f(\widehat{w})]$$

where κ ensures

$$\int_0^\infty \tilde{f}(w)\mathrm{d}w = 1$$

The modified SSVD has

$$\tilde{f}(\widehat{w}) = 0$$
$$\tilde{f}'(\widehat{w}) \approx 0$$

*Tregillis, LA-UR-18-27420

As predicted, the modified velocity distribution leads to improved voltage predictions.

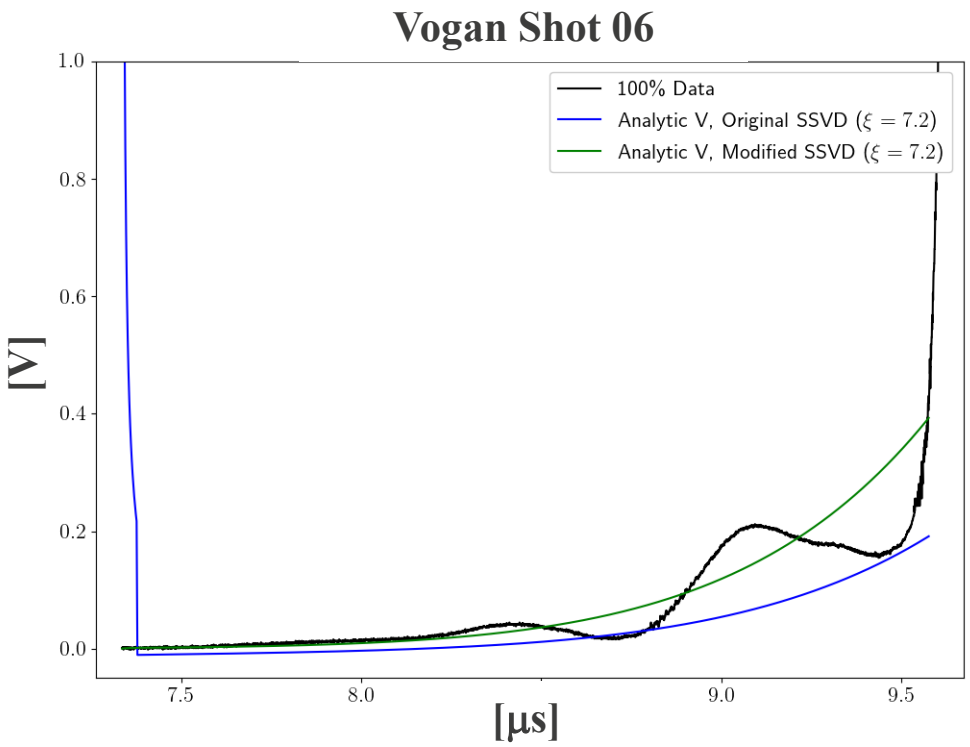

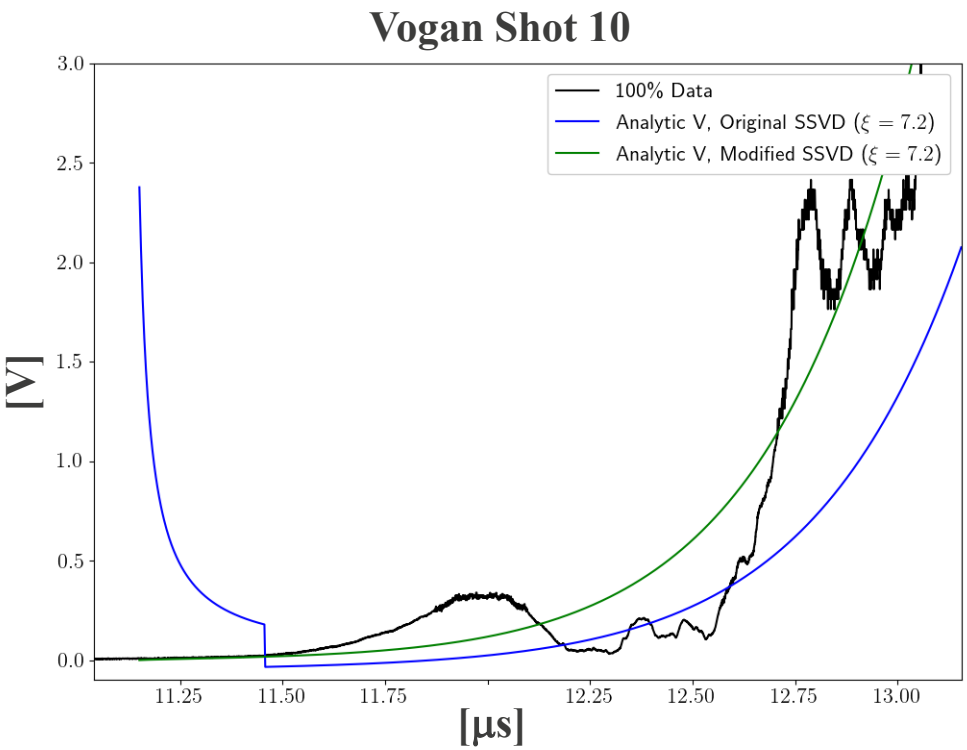

The "boundary aware" modification to the RMI+SSVD model predicts <u>continuous</u> voltage traces that rise smoothly from the baseline.

*Vogan et al. *J. Appl. Phys.* 98:113508 (2005); piezoelectric data courtesy of William Buttler.

Analytic radiographs illustrate the beneficial effect of modifying the SSVD in accordance with the boundary condition requirements.

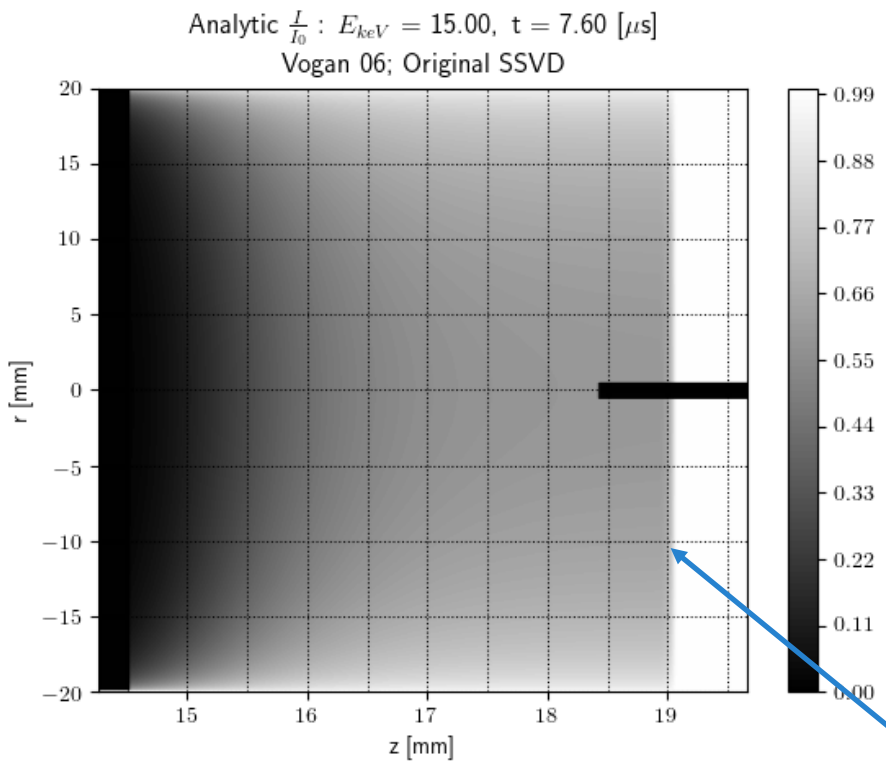

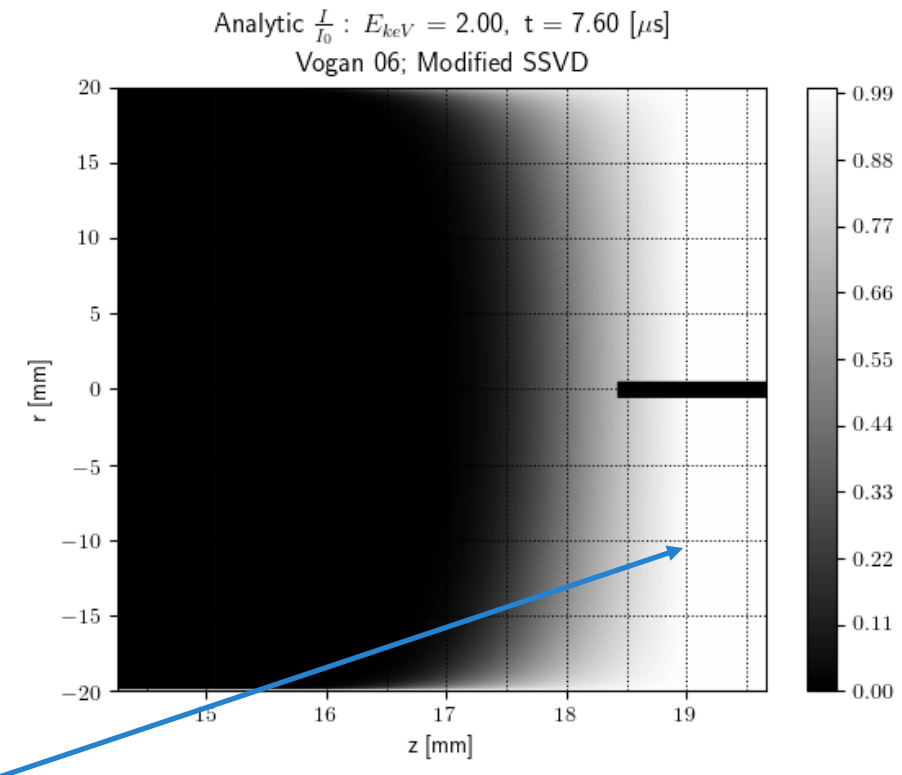

Ejecta leading edge location is the <u>same</u> in both calculations.

Original SSVD: Cloud leading edge is prominent at high energies → Hard pin impact.

Modified SSVD: Cloud leading edge is invisible at low energies → Gentle pin impact.

Recomputing the analytic mass prediction using the modified SSVD. . .

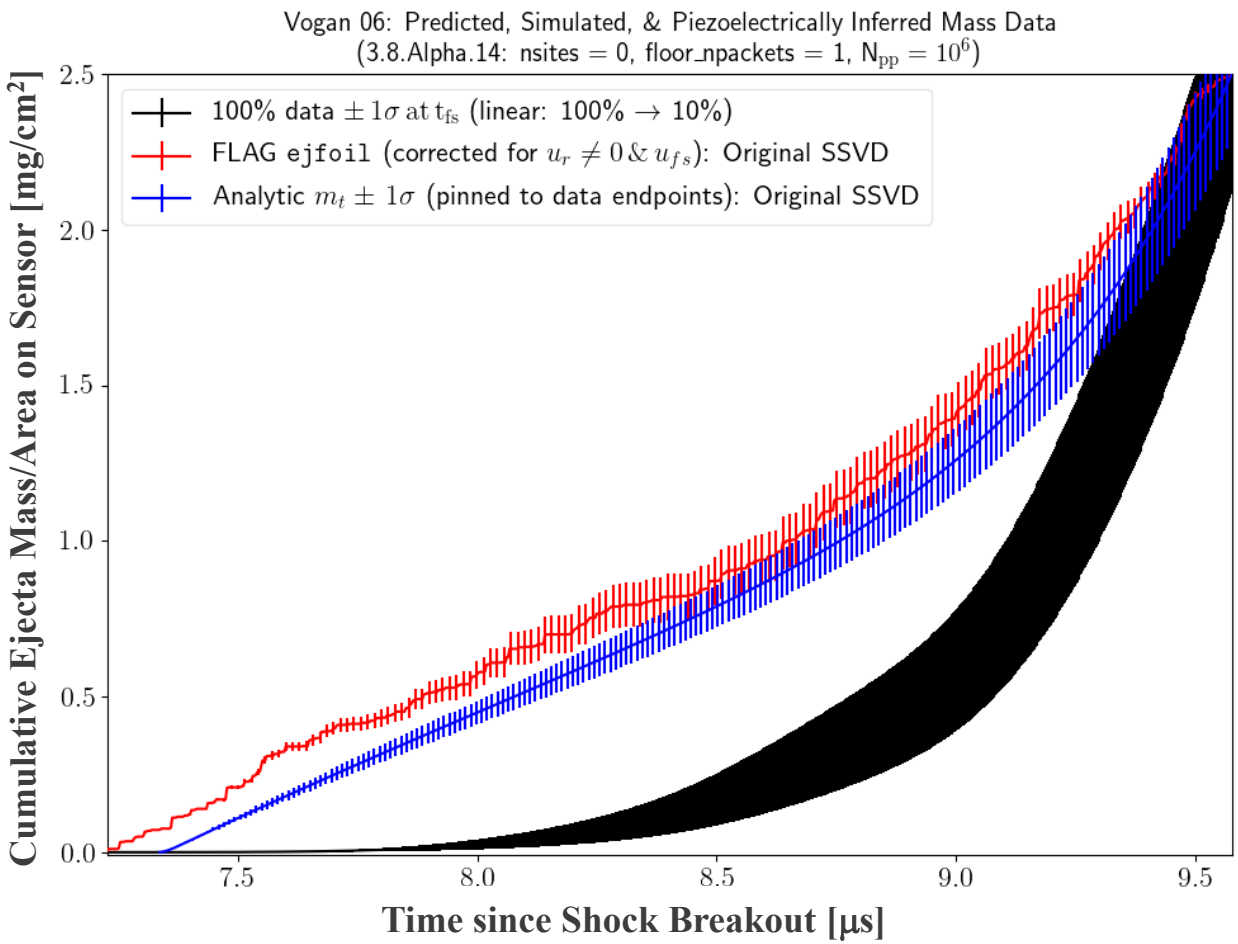

Vogan et al. *J. Appl. Phys.* 98:113508 (2005); piezoelectric data courtesy of William Buttler.

…yields a significantly improved comparison to the unthresholded data for this particular shot (Vogan 06).

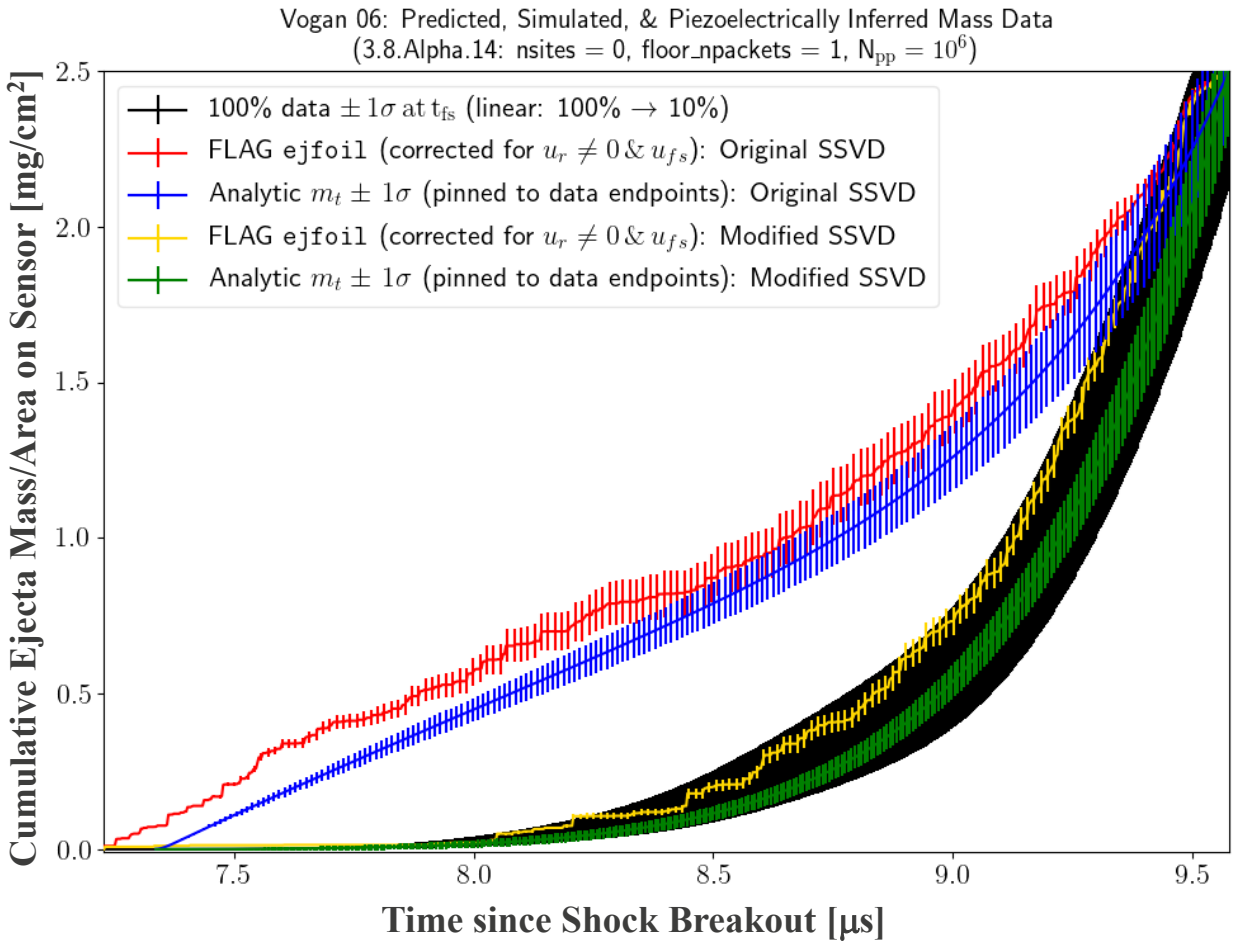

Modified SSVD	Score
Theory / 100% data	~99
FLAG / 100% data	~99

Original SSVD	Score
FLAG / 100% data	~14
Theory / 100% data	~40

The original SSVD yields

$$\dot{m}_{t,i} = 0;\ \ddot{m}_{t,i}, \dddot{m}_{t,i} \neq 0$$

The modified SSVD yields

$$\dot{m}_{t,i} = \ddot{m}_{t,i} = \dddot{m}_{t,i} = 0$$

Vogan et al. *J. Appl. Phys.* 98:113508 (2005); piezoelectric data courtesy of William Buttler.

Quantitative V & V: Our Guide to Future Efforts

Theory-simulation comparisons tell us how the code performs relative to the model, and how to improve the code.

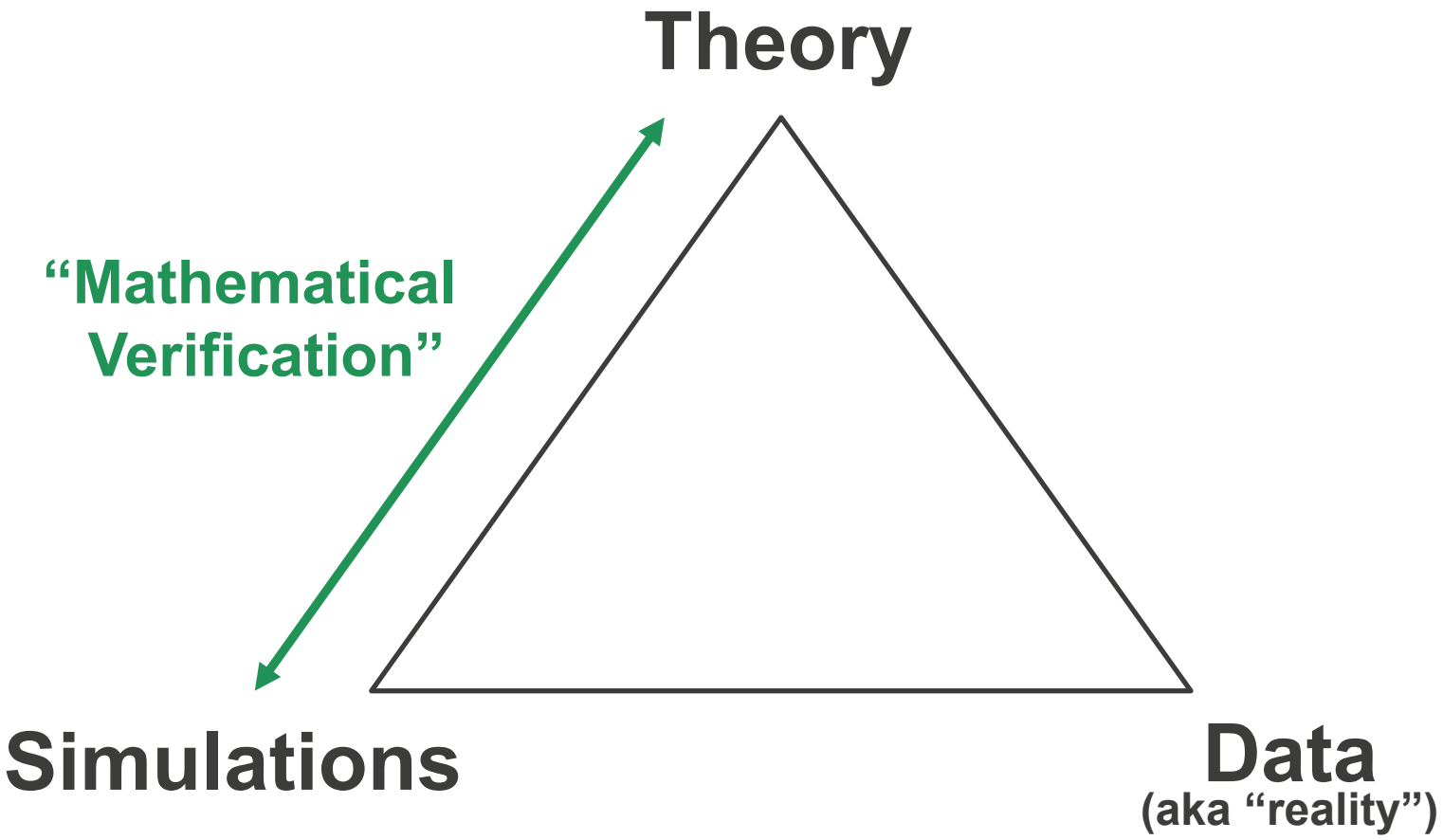

In the limit of low βτ, the FLAG calculations are an excellent representation of the theoretical predictions, but deviations grow as βτ increases (or as kh_0 decreases?)

Vogan 05

βτ = 5.12 ns, kh_0 = 1.57

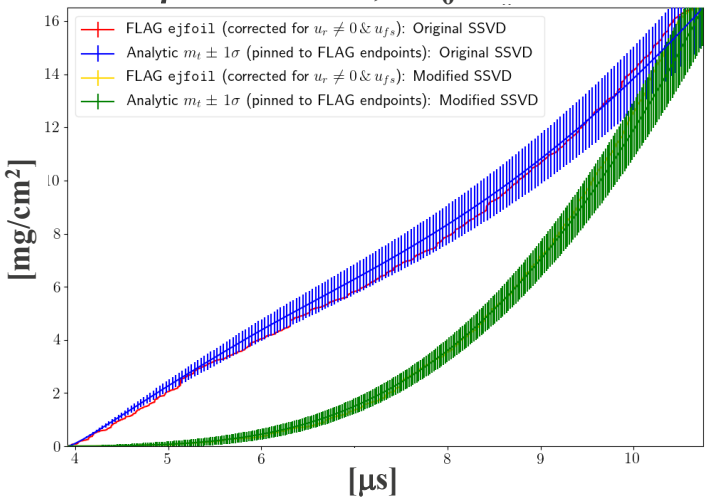

Vogan 06

βτ = 9.98 ns, kh_0 = 0.19

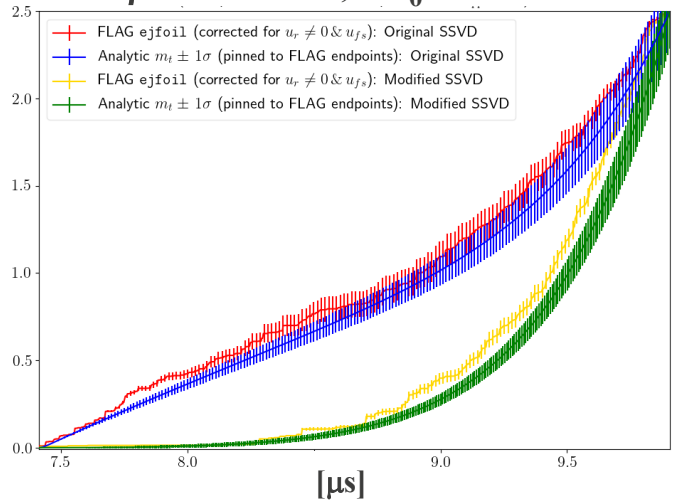

Vogan 10

βτ = 165.2 ns, kh_0 = 0.08

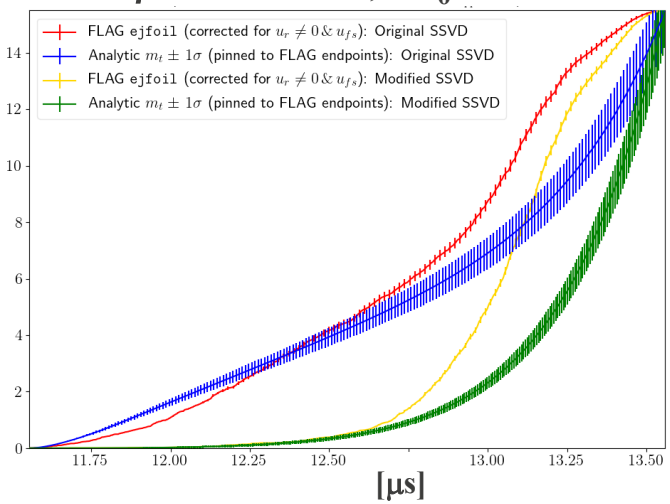

0σ on FLAG: We haven't yet analyzed the simulation error bars for Vogan 05. →

Shot	βτ [ns]	Scores, Original SSVD: FLAG / Theory	Scores, Modified SSVD: FLAG / Theory
05	5.12	~87	~99
06	9.98	~84	~40
10	165.2	~4	~18

Vogan et al. *J. Appl. Phys.* 98:113508 (2005)

Theory-data comparisons tell us how the model performs relative to the data, and how to improve the model.

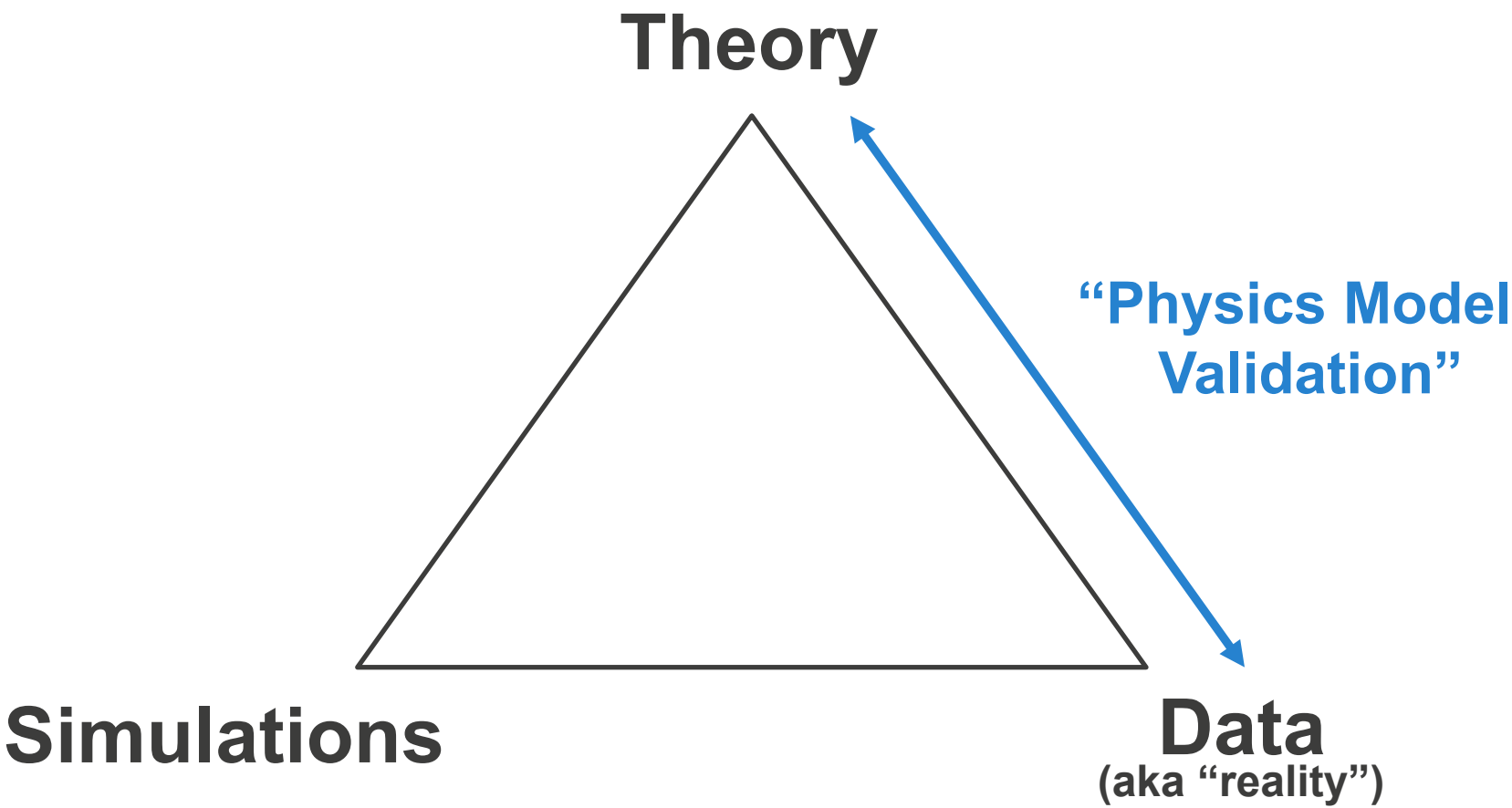

Modifying SSVD according to the boundary condition requirements substantially improves model / data compatibility.

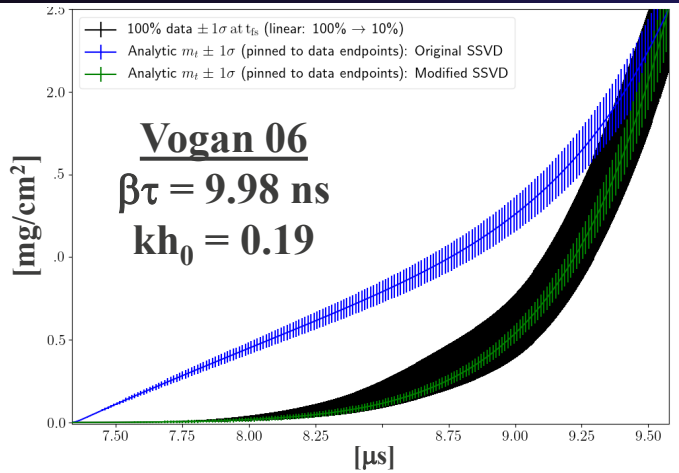

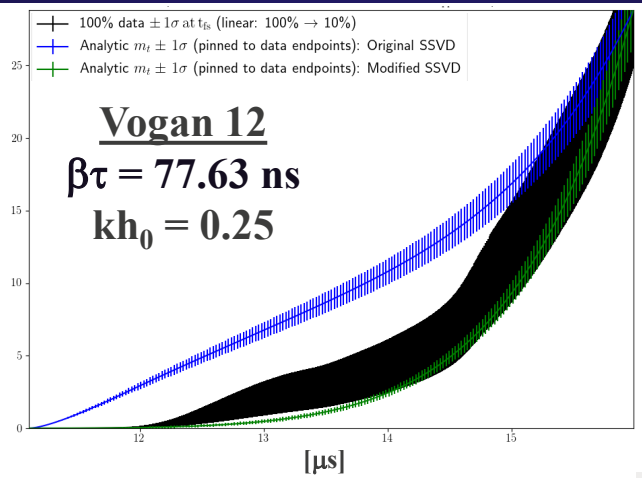

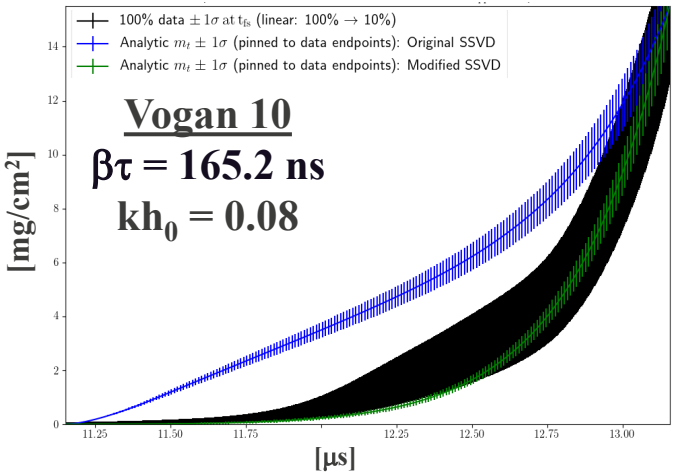

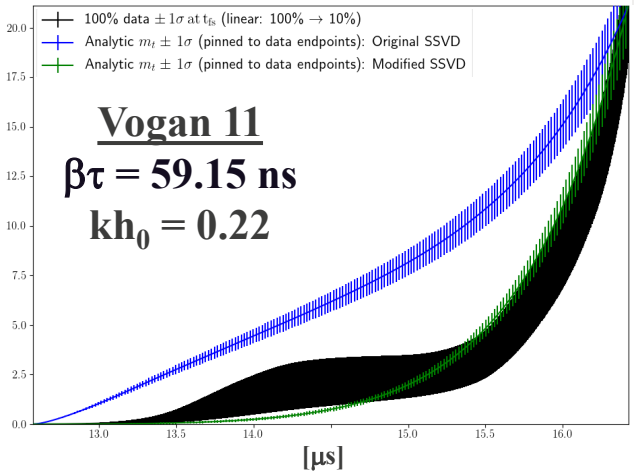

Shot	Original SSVD Data / Theory	Modified SSVD Data / Theory
06	~40	~99
10	~47	~99
11	~23	~93
12	~48	~95

Vogan et al. *J. Appl. Phys.* 98:113508 (2005); piezoelectric data courtesy of William Buttler.

But there are <u>many</u> ways to conduct the comparisons…

SSVD
ξ

Free parameter. FLAG uses 7.2, based on empirical comparison to data

Ejecta
$\dot{\eta}^s$ **or** t_{a0}

Predicted: Derived strictly from the RMI model prediction
Pinned: Pinned to the value implicit in the data (1st arrival time)

Data

Unthresholded: 100% of recorded mass domain
Thresholded: 99% of recorded mass domain

Production interval

Tuned: tuned to match the total observed mass for each shot
Prescribed: set by *ansatz**: $t_{cf} = a\,\lambda / u_{fs}$; $a = 40 \pm 10$

This yields $\pm^{10}_{8}$% variation on RMI's mass prediction.

Time-dependent data uncertainty†

Constant: 1σ uncertainty is 10% at all times
Linear: 1σ uncertainty declines linearly 100% → 10%

*Hammerberg et al. *J. Dyn. Beh. Mat.* 3:316 (2017); †See Buttler et al. *J. Appl. Phys.* 101:063547 (2007)

…so we computed the model / data compatibility score for 115,200 scenarios.

Ensemble Parameters

ξ:	400 values: $2 \le x \le 22$
data:	100% & 99%
t_{cf}:	tuned (1) & prescribed (3)
t_{a0}:	predicted & pinned to data
SSVD:	original & modified
shots:	Vogan 3-8 & 10-12

Score Calculations

data ± 1σ ("constant"); model ± 0.2σ
Narrow band on the model elucidates trends at the cost of lowered scores.

- **Modifying SSVD is more effective than thresholding the data.**
- **Model compatibility is very sensitive to the <u>unknown</u> ejecta production interval, even within the range allowed by the mass measurement uncertainty.**

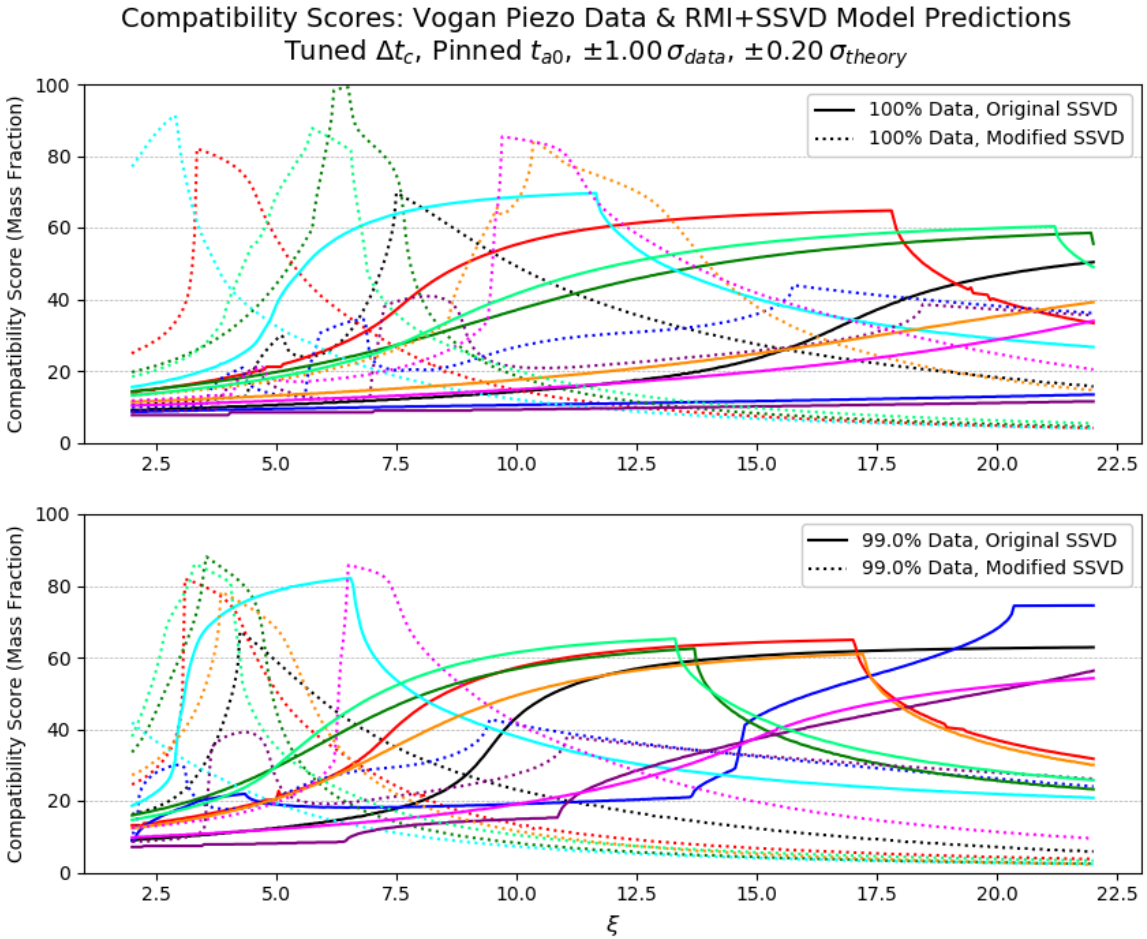

Summary: "V&V is simply the scientific method…"

- A closed-form, analytic solution exists for the RMI+SSVD ejecta source model's prediction of piezoelectric mass data in one particular class of experiments.*

- This solution ("theory") can and should be used to separate issues of verification from issues of validation when assessing the source model.

- Simulation-data comparisons provide accuracy, uncertainties, & bounds on model utility.
  – Additional work is needed to identify the causes of these uncertainties and bounds.

- Theory-data comparisons tell us how to improve the model:
  – Modify SSVD to satisfy the boundary conditions implicit in the raw voltage data.
  – Work toward physics-based prediction of the ejecta production interval.

- Theory-simulation comparisons tell us how to improve the code:
  – E.g., study the deviations from theory in the "high $\beta\tau$" or "low kh_0" regimes.

(*Planar, single-shock ejection into vacuum.)

We're faced with a few interesting but unanswered questions.

- What determines the ejecta production interval?
  - A direct measurement of the interval would be a vital test for any source model.
  - A physics model for shutoff is necessary for true predictive capability.
- What if $[\nabla \cdot \bar{u}]_r \neq 0$?
  - The piezo pin is very narrow and very far away. A small radial velocity component in the ejecta could have a large impact on the inferred mass.
- Do we need to account for perturbation shape?
  - Sine wave vs triangle wave vs. sawtooth…
  - DNS and MD calculations* suggest spike geometry varies with groove shape.
  - kh_0 may hide trends with λ & h.

*Cherne et al. *J. App. Phys.* 118:185901 (2015)